

Impact of ammonia pretreatment conditions on cellulose III allomorph ultrastructure and its enzymatic digestibility

Leonardo da Costa Sousa^{1*}, James Humpula¹, Venkatesh Balan²,
Bruce E. Dale¹, Shishir P.S. Chundawat^{3*}

¹ DOE Great Lakes Bioenergy Research Center (GLBRC), Department of Chemical Engineering and Materials Science, Michigan State University, 3815 Technology Boulevard, Lansing, MI 48910, USA

² Department of Engineering Technology, College of Technology, Biotechnology Program, University of Houston, 304A College of Technology Building, Houston, TX, 77204, USA

³ Department of Chemical and Biochemical Engineering, Rutgers State University of New Jersey, 98 Brett Road, Engineering Building Room C150A, Piscataway, NJ, 08854, USA

ABSTRACT

Plant biomasses enriched in crystalline cellulose allomorphs, like native cellulose I (CI), can be structurally altered using anhydrous liquid ammonia to form an enzymatically-less recalcitrant cellulose III (CIII) allomorph. Here, we designed and implemented an advanced ammonia pretreatment reactor/sampler setup that allowed us to systematically study the impact of several process parameters on ammonia-cellulose I complex and ultimately CIII formation, including ammonia-to-cellulose concentration, ammonia/co-solvents concentration, pretreatment time, and temperature. Pretreated cellulose ultrastructural characterization was performed using complementary X-ray Diffraction, FT-Infra Red, and Raman Spectroscopy based techniques. We found that the amorphous content of cellulose increased initially when the intermediate ammonia-cellulose I complex was formed within the first 30 seconds of pretreatment. But a reduction in the amorphous content was observed if the complex was annealed for longer periods of time and/or at high temperatures, resulting in a highly crystalline and well-ordered CIII allomorph. However, depending on the exact pretreatment conditions tested, CIII-‘like’ cellulosic substrates with varying allomorphic ultrastructures and crystalline-order were formed. Interestingly, CIII-‘like’ allomorphs with higher crystallinity were more easily hydrolyzed by cellulase enzymes compared to native CI and lower crystallinity CIII-‘like’ substrates. This work highlights the challenges associated with systematically conducting ammonia treatments, interpretation of CIII ultrastructure using appropriate analytical techniques, and the influence of cellulose ultrastructure on enzymatic digestibility in light of previous work. Lastly, we explored reduced severity and more cost-effective pretreatment conditions that could lower recalcitrance of cellulose by

* Corresponding Authors:

Shishir P.S. Chundawat (Email: shishir.chundawat@rutgers.edu; Phone: +1-848-445-3678); Department of Chemical and Biochemical Engineering, Rutgers, The State University of New Jersey, 98 Brett Road, Engineering Building Room C150A, Piscataway, NJ, 08854, USA) and Leonardo da Costa Sousa (Email: sousaleo80@gmail.com) DOE Great Lakes Bioenergy Research Center (GLBRC), Department of Chemical Engineering and Materials Science, Michigan State University, 3815 Technology Boulevard, Lansing, MI 48910, USA.

producing crystalline CIII and enable adoption of more advanced ammonia-based pretreatments in cellulosic biorefineries.

KEYWORDS

Cellulose Allomorphs, Ammonia Pretreatment, Cellulose Crystallinity, Cellulases, Biofuels

INTRODUCTION

One of the major bottlenecks associated with biological conversion of lignocellulosic biomass to fuels and chemicals originates from the recalcitrance of tightly packed non-covalently bonded cellulose microfibrils towards enzymatic hydrolysis.¹⁻³ This naturally occurring crystalline arrangement of cellulose in plant cell walls, denoted as cellulose I (CI), is highly resistant to hydrolysis by cellulolytic enzymes into fermentable sugars.⁴⁻⁶ However, amorphous cellulose (AC) and some non-native forms of crystalline cellulose are known to be generally more readily digestible during hydrolysis by non-complexed fungal cellulases,^{3,7,8} bacterial cellulosomal complexes,⁹ and some cellulolytic¹⁰ microorganisms. For example, Chundawat et al. (2011) and Cui et al. (2014) have both shown that amongst crystalline cellulose allomorphs, cellulose-III is significantly more digestible by fungal cellulases to fermentable sugars compared to both cellulose-II and cellulose-I.^{3,11} Wada et al. (2010) have shown that cellulose-II hydrate is significantly more digestible by fungal cellulases than freeze-dried cellulose-II and native cellulose-I. While Mittal et al. (2011) has shown that freeze-dried cellulose-II has higher rates of enzymatic digestion compared to other cellulose allomorphs likely due to increased amorphous cellulose content.^{8,12} Chundawat et al. (2011) converted plant-derived CI from Avicel PH-101 into cellulose III (CIII) using anhydrous ammonia, thereby improving enzymatic hydrolysis rates for synergistic fungal cellulase cocktails nearly two fold compared to native CI.³ Igarashi et al. (2007) had also observed that CIII derived from algal-derived cellulose had an increased enzymatic hydrolysis rates for processive cellulolytic enzymes,¹³ which is now thought to arise largely due to increased endo-exo synergistic activity of cellulases.^{3,14} The mechanistic reasons for such activity improvements are still far from being fully understood from an enzyme-perspective.^{3,14,15} On-going research over recent years has unveiled interesting phenomena at play that leads one to question the several established paradigms regarding mechanisms of enzymatic hydrolysis of crystalline cellulose. For example, Gao et al. (2013) observed that fungal cellulases tend to bind less tightly to CIII versus CI, even though their overall synergistic endo-exo activity is higher on CIII.¹⁴ Molecular dynamics simulations of various cellulose allomorphs suggest that this enhancement in cellulase activity likely originates from favorable free energies during decrystallization of individual cellulose chains from the crystal surface,¹ as well as intrinsic kinetic factors related to processivity of productively bound enzymes to the non-native allomorph.^{3,14,15} However, the relationship between relative binding affinity and hydrolytic activities of fungal cellulases on CIII with varying degrees of crystallinity is still poorly understood due to the inherent challenges associated with preparation of well-defined CIII substrates under controlled ammonia pretreatment conditions. This is further complicated by the lack of consistency in the calculated crystallinity indices when comparing between distinct cellulose allomorphs using different analytical techniques like XRD versus NMR.^{8,16} This is particularly problematic even when making comparisons between allomorphs using XRD based crystallinity index values alone, particularly for samples with a high degree of disorder associated with the cellulose polymers (e.g.,

see Table 4 in 2011 Mittal paper⁸ for anomalous results for cellulose-II compared to other allomorphs when crystallinity index is determine using XRD versus NMR). This has made it challenging to also clearly quantify what is ‘amorphous cellulose’ (AC) using XRD alone and if all forms of amorphous cellulose are structurally equivalent or even impact enzymatic activity in a similar manner.

Several researchers have studied the factors that impact ammonia pretreatment conditions on CIII formation and crystallinity over the last eighty years.^{8,17,18} Liquid anhydrous ammonia and primary amines have been successfully used as swelling agents of cellulose, as they intercalate into the crystalline structure of cellulose disrupting the native hydrogen bonding network to form a metastable, swollen cellulose-ammonia (or amine) complex.¹⁸⁻²¹ CIII is formed from these swollen cellulose-ammonia complexes upon removal of ammonia (or amine) from the above-mentioned swelling agents.^{18,19} Since ammonia is a volatile alkali it provides unique advantages for producing pretreatment catalyst/solvent free pretreated biomass as compared to other leading pretreatment processes.²² Ammonia has been also used most commonly in the literature as a swelling agent for inter-conversion of CI into CIII via this intermediate cellulose-ammonia complex. Ammonia pretreatment has been performed at various operating conditions that includes its usage in supercritical state or sub-critical liquid state at close to ambient pressures.^{13,19} The effect of temperature during ammonia treatment and co-solvent polarity during ammonia removal from the swollen cellulose-ammonia complex are well known factors impacting conversion of CI into CIII and AC.^{8,18,19,23,24} Higher annealing temperatures during ammonia treatment and/or during ammonia removal from the ammonia-cellulose complex can significantly increase the crystallinity indices (CrI) of the CIII produced that is stable in hot water.²⁴ While sometimes extended ammonia treatment times are reported to reduce CrI (and produce significant fraction of AC) even at higher treatment temperatures.¹⁹ But as first clearly shown by Yatsu and co-workers both temperature and pressure play a critical role in the formation of a stable crystalline CIII allomorph.²⁴ It is very likely that the ambiguity in the literature about stable CIII formation conditions is likely exacerbated by the lack of suitable tools/know-how to safely and properly handle pressurized ammonia at well-defined temperature/pressures to conduct ammonia-based pretreatments. Yatsu clearly showed that treatment of cellulose with ammonia at room temperature but removal of ammonia under partial vacuum (~20 millitorr) resulted in hardly any conversion of CI to CIII. However, increasing the pressure close to 100 psi or higher during ammonia removal from the cellulose-ammonia complex even at ambient temperatures allows significant conversion of CI into CIII. This finding is also supported by the fact that ammonia in its gaseous state is unable to convert CI into CIII. Furthermore, ammonia removal under non-pressurized conditions results in highly decrystallized cellulose (also sometimes reported in the literature as ‘AC’) with marginal formation of CIII as indicated by XRD.²⁴ Due to lack of a well-defined structure of ‘AC’ by its very definition and lack of experimental tools to better characterize cellulose ultrastructure other than using powder XRD and solid-state NMR, the formation of amorphous or disordered cellulose formed during ammonia based pretreatments has been challenging to study. Recently molecular dynamics (MD) simulation studies have also suggested that ammonia can fairly instantaneously cause structural changes in the CI crystal fibers, creating a modified disordered crystal with channels created that only then facilitate ammonia penetration and finally produce a fully swollen cellulose-ammonia complex.²⁵⁻²⁷ But, it has not been possible to test this hypothesis experimentally, or monitor the initial disordered amorphous-like state of cellulose, since most

ammonia pretreatments are done on the order of several minutes or hours with the lack of a suitable experimental setup to be able to successfully trap such intermediate states formed during CI treatment, particularly during the first few minutes of pretreatment with precise control over the pretreatment conditions. The next question to ask is if all forms of disordered or amorphous cellulose are created equal, and if obviously not, then how do we characterize these substrates? One additional practical approach is to test the enzymatic digestibility of these different substrates to identify substrates and associated pretreatment conditions that produce pretreated cellulose allomorphs that are better suited for industrial processing by commercial enzymes.

Mittal and co-workers (2011), inspired by the classical protocol first reported by Barry and co-workers,¹⁸ have reported an ammonia pretreatment protocol that cycled the cellulose pretreatment temperature starting from -75 °C using a dry ice/acetone bath to first condense and contact cold liquid ammonia with cellulose before raising the reactor temperature. They report then raising the temperature from -75 °C slowly up to -33 °C (close to boiling point of ammonia) at 1 atm and then up to 25 °C or higher temperatures (under pressurized conditions using a Parr reactor) for various durations of time. This is followed by complete removal/evaporation of the ammonia from the swollen cellulose-ammonia complex via rapid depressurization and venting of the pretreated samples in a fume hood to produce CIII of varying degrees of crystallinity.⁸ However, due to the lack of control over the exact pretreatment temperature, total treatment time, and ammonia removal conditions we still have a poor understanding of how subtle variations in the ammonia pretreatment conditions can impact CIII crystallinity. Furthermore, as reported in this previous study and in our current work, subtle variations in the ammonia treatment conditions can indeed result in the formation of CIII like allomorphs with only slight differences in the underlying cellulose ultrastructure (as detected using standard XRD or NMR based methods) that significantly impacts enzymatic saccharification susceptibility. For example, rapid depressurization of ammonia from the reactor during ammonia removal can cause the pretreated sample temperature to drop rapidly close to -33°C (at 1 atm), depending on the exact ammonia/cellulose loadings and ammonia removal rate, which makes it challenging to assign a well-defined treatment temperature (without temperature cycling) using the conventionally reported methods. Temperature cycling alone during ammonia-based pretreatments can cause significant changes in the cellulose structure^{28,29} and therefore should be ideally avoided to generate a well-defined CIII allomorph of defined crystallinity and ultrastructure. Lastly, a better understanding of the exact pretreatment conditions that give rise to a pretreated cellulose-III allomorph with desired susceptibility towards cellulases is still needed to develop commercially relevant ammonia-based pretreatment processes. Currently most commonly referred to processing conditions in the literature are either very energy intensive (i.e., supercritical ammonia treatment),³⁰ or require extensive temperature cycling and ultra-low temperatures during operation,^{8,18} and are not optimized for formation of a well-characterized CIII allomorph from the context of generating an easily digestible cellulosic substrate in a biorefinery setting.³¹ Ideally, the most favorable conditions would be to perform ammonia pretreatments at constant (or non-cycling) conditions that are preferably close to ambient temperatures/pressures, thereby reducing the total operating and capital costs due to milder operating pressures/temperatures theoretically required for running such operations.²²

Here, a systematic understanding of how ammonia pretreatment conditions (e.g., temperature, swelling time, ammonia-to-cellulose loading, quenching solvent etc) impacts CI to CIII conversion

was conducted using a new type of ammonia pretreatment reactor/sampler assembly. Here we revisit the controversial question regarding the relationship between XRD predicted crystalline CIII content (vs. disordered or amorphous cellulose content) and the substrates enzymatic hydrolysis rate using commercially relevant fungal cellulase cocktails. This is made possible using a novel ammonia pretreatment and ammonia removal reactor setup, multifaceted cellulose ultrastructure characterization (e.g., using FTIR, XRD, and Raman Spectroscopy), and finally using a standard XRD based quantification of the relative crystallinity index of CIII produced under various controlled pretreatment conditions to compare to previous work. Moreover, in addition to varying the ammonia pretreatment variables (i.e., temperature, time, ammonia loading), the impact of polar and non-polar co-solvents (e.g., water, ethanol) either during the ammonia pretreatment process or during ammonia removal to form CIII was also evaluated here. Overall, this study improves our understanding of how well-controlled ammonia based pretreatments can impact cellulose structure, explore the non-trivial relationship between distinct CIII substrates with varying crystallinity possibly formed during ammonia treatment and their relative enzymatic digestibility, and provide impetus towards development of more cost-effective extractive ammonia (EA)³² based pretreatments for next-generation cellulosic biorefineries.

EXPERIMENTAL SECTION

Ammonia pretreatment reactor setup

A novel pretreatment reaction apparatus was custom designed and assembled to convert cellulose I (CI) into cellulose III (CIII) under controlled pretreatment conditions. Details regarding the experimental setup used for pretreatment and associated process schematic labels are provided in the supporting information (SI) document (Fig. S1). As shown in Fig S1, the apparatus consisted of two major sections that include ammonia delivery system (labels 1-6) and pretreatment reaction/sampling equipment (labels 7-12). As it was important to accurately deliver the appropriate amounts of ammonia at set-point temperature, an ammonia preheating vessel (1 – Parr Instrument Company, Moline, IL, USA) equipped with temperature controller (2) was installed on the top of a balance (5 – A&D, Inc., San Jose, CA, USA). This balance was used to measure the displaced weight of ammonia from the preheating vessel to the reactor by a jacketed syringe pump (4 – Teledyne Isco Model 500D, Lincoln, NE, USA). To avoid heat losses during ammonia delivery, the syringe pump jacket was temperature controlled by a circulating water bath (3 – VWR, Radnor, PA, USA). Ammonia was delivered to the reaction vessel (7 – HEL, Inc., Hertfordshire, UK) at constant pressure with the help of a backpressure regulator (6 – Parker, Cleveland, OH, USA). An online temperature PID controller (8 – Julabo, Seelbach, Germany) was installed to maintain the desired temperature during reaction time. Reaction pressure was controlled by HEL, Inc. software (12) actuating two solenoid valves (9 and 10) for nitrogen inlet and outlet, respectively. Reaction temperature and mixing controls were also activated via computer software designed by HEL, Inc. (12). Cellulose suspensions were sampled through a valve connected to a dip tube (11) that was installed at the top of the reaction vessel under desired sampling conditions. Unless noted otherwise, commercial grade anhydrous ammonia (>99.5% purity from Airgas, Lawrenceville, GA) was used for all studies. Analytical grade Acetone and Methanol were procured from Sigma-Aldrich and 200 Proof Ethanol was procured from VWR Scientific. A wide range of pretreatment conditions were next tested using this reactor setup as outlined in the SI document methods section M1 to M4, such as varying (M1) ammonia-cellulose

complex sampling or quenching solvent, (M2) ammonia to cellulose loading, (M3) temperature and time of pretreatment, and (M4) ethanol:ammonia co-solvent concentration.

Cellulose ultrastructure characterization using XRD, FTIR, and FT-Raman

Details regarding the X-ray powder diffraction (XRD) method and data analysis technique to estimate cellulose crystallinity, using the amorphous subtraction and peak deconvolution methods, are provided in the SI document supporting methods section M5.^{16,33} Note that, similar to previous work,³⁴ XRD equatorial reflections for (101), (10 $\bar{1}$), and (002) crystallographic planes for native CI standard were at approximately 14.9°, 16.3°, and 22.5° Bragg angles (θ), respectively. Equatorial reflections for (101), (10 $\bar{1}$), and (002) crystallographic planes for CIII standard were at approximately 11.7°, 17.1°, and 20.6° Bragg angles (θ), respectively. Additional supporting details regarding the FT-IR (Infra-Red) and FT (Fourier Transform)-Raman based spectroscopic characterization methods are provided in the SI document supporting methods section M6 and M7, respectively.

Preparation of pretreated cellulose standards

High purity (>98% cellulose content, dry weight basis or dwb) microcrystalline CI, purchased from Sigma-Aldrich (Avicel PH-101, Lot No. BCBD6923V). This sample also served as CI standard used in this study for quantitative XRD analysis method outlined in the SI document. While, the CIII standard for quantitative XRD analysis was produced from Avicel PH-101 using liquid anhydrous ammonia, prepared in a high-pressure stirred batch reactor at 90 °C for 30 min residence time (starting at the exact time the ammonia was first contacted with the biomass), using a 6:1 ammonia-to-cellulose loading ratio (dwb). The CI sample had a total moisture content less than 4-5% (twb) and was used directly for all ammonia pretreatment studies without any further drying. The reactor pressure was maintained constant at 1000 psi using nitrogen gas. After completing the reaction for the desired time, ammonia was slowly evaporated from the reactor through a venting valve. During this process, the temperature of the reactor was slowly decreased due to heat of vaporization of ammonia and was stabilized at 25 °C with a heating controller. After reaching atmospheric pressure, the cellulose sample was removed from the reactor, transferred to a flat container and placed overnight in the fume hood to evaporate residual ammonia. No visual differences in color were observed after ammonia treatment of cellulose at these conditions leading to the assumption that there was minimal interference from Maillard-type reaction products on downstream enzymatic assays.^{3,35} The CIII standard for XRD analysis was stored at 4 °C in a zip sealed bag prior to usage. The amorphous cellulose (AC) standard was produced using phosphoric acid treatment of Avicel PH-101 as described in the literature.^{36,37} Phosphoric acid swollen cellulose (PASC) was freeze-dried and stored at 4 °C in zip sealed bags prior to further usage. Samples used as standards for XRD quantitative analysis were also characterized by FTIR and FT-Raman spectroscopy to get detailed structural information.

Enzymatic hydrolysis and purified protein-cellulose allomorphs adsorption/binding assays

Cellulose samples were subjected to enzymatic hydrolysis at 1% glucan loading in 10 ml reaction volume using 15 ml glass vials as described elsewhere,³ based on the original NREL protocols.³⁸ The total protein loadings used during reaction were either 4.0 or 7.5 mg/ g glucan of Accellerase 1500 enzymes (DuPont, formerly Genencor, Palo Alto, CA, USA). The protein concentration (84 mg/ml) for the enzyme stock solutions was determined using the Kjeldahl nitrogen analysis

method as described elsewhere.³⁹ When 4 mg enzyme/g of glucan was used, sugar yields were evaluated for 24 h residence time, while for 7.5 mg/g glucan, enzymatic hydrolysis was evaluated for 4 h hydrolysis time. In all assays, final reaction volume pH was adjusted to 4.8 using sodium citrate at 50 mM buffer concentration prior to incubation of the glass vials at 50 °C in an orbital shaking incubator set at 200 RPM (New Brunswick, Innova 44, Enfield, CT, USA). The supernatant from the reaction volume was filtered through a 0.45 µm filter and subjected to HPLC analysis. Monomeric glucose was quantified using a Shimadzu HPLC system equipped with an Aminex HPX-87H carbohydrate analysis column (Biorad, Hercules, CA) and Waters 410 refractive index detector (RID). Degassed HPLC grade water with 5 mM H₂SO₄ was used as a mobile phase at 0.6 mL/min. Injection volume was 20 µL with a run time of 20 minutes. Glucan conversion to glucose was quantified as described in the NREL protocol.³⁸ All hydrolysis assays were carried out in duplicate with mean values for glucan-to-glucose conversion reported here. Error bars shown indicate standard deviations ($\pm 1\sigma$) for reported mean values. Lastly, Green Fluorescent Protein (GFP) labeled type-A Carbohydrate-Binding Module (CBM) protein production and protein-cellulose binding assay details are briefly provided in the SI document supporting methods section M8.

RESULTS AND DISCUSSION

Effect of sampling or quenching solvent on cellulose III formation: The mechanism for converting CI to CIII, as originally proposed by Schuerch (1963),⁴⁰ involves penetration of anhydrous liquid ammonia into the cellulose crystal, followed along with the disruption of the native cellulose hydrogen bonding network. This results in creation of a metastable crystalline complex with a larger unit cell than CI,^{27,41} and was designated as the ammonia-cellulose complex. Upon removal of ammonia from this complex, the inter-chain/intra-chain cellulose hydrogen-bonding network is rewired in a distinct pattern from native CI, generating a new crystalline allomorphic form designated by CIII. During this operation of ammonia removal, the heat of vaporization of ammonia is often large enough to reduce the surface temperature of the cellulose fibers to well below 0 °C impacting the reproducibility of the process and causing thermal-cycling of the samples during ammonia evaporation. As described by Lewin et al. (1971),¹⁹ the temperature at which CIII is formed, i.e., during ammonia evaporation, can affect the crystallinity of cellulose. Therefore, it is necessary to control this parameter during the pretreatment process to avoid misleading interpretation of experimental results. For this purpose, a “heat sink” composed of a large volume of sampling or quenching solvent was used to facilitate ammonia removal in this study (see Fig. S1). The ammonia-cellulose complex, suspended in liquid ammonia, was first carefully sampled from the high-pressure reactor into a “heat sink” prior to ammonia removal. The cellulose sample was further filtered and washed extensively with the same solvent to remove residual ammonia before being dried in the fume hood overnight (to remove residual solvent) at room temperature. Several sampling solvents like acetone, ethanol, water, and methanol were evaluated as sampling solvents in this study. The ammonia-cellulose complex was first generated using Avicel PH-101 and pressurized liquid ammonia at 90 °C with 6:1 ammonia-to-cellulose ratio for 20 min. The glass vials containing the sampling solvents were also kept at 25 °C in a temperature-controlled water bath. After addition of the ammonia-cellulose complex to the glass vial, the ammonia evaporated slowly from the solvent without allowing the temperature to decrease below 20 °C for all cases studied. Therefore, all the solvents tested herein could potentially be used to control temperature during annealing/assembly of the CIII crystalline allomorph from the cellulose-ammonia complex.

However, the presence of a sampling or quenching solvent can also affect the annealing of CIII crystals and the final crystallinity of the sample. Therefore, we evaluated the differences between the CIII generated using various solvents tested herein to select one that offered minimal interference to CIII formation and/or the expected improved impacted enzymatic digestion.

By performing XRD on the treated cellulose samples (see **Fig. 1**), it was possible to observe differences in CIII formation as a function of the sampling solvent used. CIII formation was evaluated based on XRD based crystallinity index (CrI) measurements, which were performed according to the amorphous subtraction method (described in the experimental and supporting information file). The range of CrI values available in the literature for Avicel PH-101 can vary significantly between ~40% to ~90%, depending on the calculation method.^{16,42} Amorphous subtraction methods usually result in crystallinity indices between ~60% and ~75% for Avicel PH-101.^{16,42} However, the CrI result obtained here for CI was ~50.1%, which was slightly lower than reported literature values (see Fig. S5-S6 and SI document section M5 for details). This difference could be attributed to differences in the cellulose batch used in this study. In any case, as these values of CrI are not always consistent in the literature, our analysis was focused on the relative CrI differences between the various samples generated in this work using the same Avicel PH-101 batch. The XRD data shown in **Fig. 1** clearly reveals the importance of the sampling or quenching solvent environment that could either promote or impede CIII formation. Amongst the various organic solvents used in this study, we found that ethanol gave the highest conversion of the ammonia-cellulose complex into to crystalline CIII. This result was also correlated with the marginally higher enzymatic hydrolysis yields, by 5-8% in absolute hydrolysis yield (**Fig. 1_i**), seen for ethanol sampling based CIII as compared to other solvents used (or directly air-drying the complex). Methanol also provides a better environment for CIII formation from the complex compared to using acetone or direct air drying, which generated similar results. The reasons behind these differences are yet to be fully understood and more work is necessary (e.g., molecular dynamics simulations) to clarify the role of solvents on cellulose-ammonia complex stability and conversion to CIII. As ethanol was the most effective sampling media for CIII conversion, it was the ideal sampling solvent used for all subsequent experimental work reported here.

The most distinctive result was obtained when we sampled the ammonia-cellulose complex directly into water. The sample generated after removal of water and ammonia resulted in a substrate with poorly defined XRD that could not be effectively deconvoluted by the amorphous subtraction method described earlier. Therefore, this suggests that this sample of low crystallinity cannot be simply described as a mixture of solely CI, CIII, and AC. Also, since the enzymatic digestibility of highly amorphous PASC has been shown to be significantly higher than crystalline CIII,^{3,14} it is clear that PASC is also likely more digestible than the low crystallinity CIII sample generated after sampling the ammonia-cellulose complex in water. These results clearly suggest that water interferes with rewiring of the cellulose hydrogen bonding once ammonia is removed from the ammonia-cellulose complex. This creates a recrystallized but disordered cellulose lacking long-range atomic order that is reflected in the poorly-defined diffraction peaks often seen for highly amorphous substrates like PASC (**Fig. 1_ii_b**). Lewin et al. (1971),¹⁹ performed a similar experiment with cotton cellulose, reporting a complete reversion to CI after drying the sample at 65 °C. Others studies conducted by Barry et al. (1936)¹⁸ and Clark et al. (1937)²¹ also revealed that aqueous ammonia treatment is able to revert CIII back to CI, after drying at 105 °C. The cellulose source (i.e., degree of polymerization and crystallite size) and sampling/drying method used by these studies are two major differences in contrast to our work presented herein, where

Avicel PH-101 was used as the cellulose source and freeze drying was used as the preferred method to remove water from the sample prior to XRD analysis. The rationale behind this choice of drying process was purposely to minimize reversion of CIII back to CI, as our preliminary evaluation revealed that freeze drying does not allow reversion of fully converted CIII to CI and has a minimal impact on the final cellulose crystallinity [data not shown].

Enzymatic digestion of the water-sampled cellulose-ammonia complex substrates resulted in significantly lower hydrolysis yields compared to cellulose-ammonia complex substrates sampled in organic solvents. Even though the former substrate has significantly lower crystallinity and is much more disordered than the later. This observation is not concordant with the current paradigm that less crystalline cellulose substrates always give rise to higher enzymatic hydrolysis rates.⁴³ The definition of AC as being a substrate with little or no ordered structural organization (discernible by XRD or solid-state NMR type techniques) can contribute to the misleading idea that all AC is created equal. However, the current observation suggests that this paradigm cannot be readily applied to non-native cellulose allomorphs like CIII and related intermediates. Similarly, another related observation is that higher CIII crystallinity resulted in improved enzymatic digestion rates, which usually is not observed for native CI.⁴³⁻⁴⁵ The role of CIII crystallinity on interaction with cellulolytic enzymes was further explored in this study by varying other pretreatment conditions to generate CIII with varying CrI as estimated via XRD. While absolute CrI measurements do not always provide a clear indication of the relative enzymatic digestibility amongst different cellulose allomorphs, due to the lack of suitable alternatives, we have used XRD predicted CrI values to allow the reader to have an absolute benchmark to compare our results with published work. This is further complemented with additional cellulose structural characterization using FT-IR and FT-Raman Spectroscopy.

Effect of ammonia loading on cellulose III formation: Ammonia loading is one of the key factors contributing to the technoeconomics and effectiveness of ammonia-based pretreatments for conversion of lignocellulosic biomass to biofuels.^{46,47} Most ammonia-based pretreatments reported in the literature use aqueous or concentrated ammonium hydroxide solutions at elevated temperatures to pretreat biomass. Although such pretreatment conditions have been reported to partially decrystallize cellulose fibers,⁴⁷ the presence of elevated concentrations of water is known to inhibit formation of the cellulose-ammonia complex that converts ultimately to CIII. Efficient conversion of CI to CIII requires contact of the cellulose fibers with liquid anhydrous ammonia at an ammonia-to-cellulose loading ratio that impacts both the rate of liquid ammonia penetration into cellulose fibers and also on the total number of hydrogen bonding sites along the cellulose chain that are simultaneously activated by ammonia. Incomplete formation of the ammonia-cellulose complex will affect cellulose III formation and ultimately lower the enzymatic hydrolysis rate of the pretreated substrate. As ammonia usage also has economic implications for a commercial-scale biorefinery, it is important to optimize the ammonia loading to efficiently convert CI to CIII using a minimum ammonia-to-biomass loading ratio.³² To determine the minimum ammonia loading that allows efficient CIII formation, anhydrous ammonia was contacted with CI at various ammonia-to-cellulose ratios ranging from 1:1 to 6:1 (w/w; dwb). In **Fig. 2**, one can inspect (i) the extent of CIII formation as determined by XRD, and (ii) the impact on enzymatic hydrolysis yields for substrates prepared for this range of ammonia loadings. From the XRD spectra presented in **Fig. 2**, it is evident that ammonia-to-cellulose ratios of 1:1 and 2:1 are not sufficient to completely modify the native crystal state of cellulose even after 10 min of

treatment time. Efficient conversion of CI to CIII is only observed at ammonia-to-cellulose ratios greater than or equal to 3:1. From the XRD spectra, it is also clear that the CIII peaks are sharper and taller for 6:1 than 3:1 ammonia loading, leading to a marginally more crystalline CIII in the former. These results confirm that higher ammonia loadings can improve the mass action responsible for efficient penetration of ammonia in the cellulose crystal, being able to activate cellulose to produce ammonia-cellulose complexes more effectively than at lower ammonia loadings. It is possible that for the lower ammonia loadings, some hydrogen bonding sites are still not fully activated by ammonia within the first 10 min of treatment time, leading to an incomplete annealing of cellulose chains during ammonia removal that results in lower CIII crystallinity (and/or presence of unconverted native CI). For ammonia-to-cellulose ratios greater than 6:1 (e.g., up to 20:1) it was not possible to observe any significant changes in CIII formation (data not shown), suggesting a saturation effect at ammonia loadings around 6:1. Therefore, this was the maximum ammonia loading used subsequently in this study. Other studies have reported the successful conversion of CI to CIII using ammonia loadings between 2:1 and 3:1 for longer treatment times (30-90 min), while ramping down the temperature first to -75 °C and then increased slowly to 25 °C or higher to remove the ammonia.⁸ Also, literature reports show that it is possible to achieve high CIII conversion with ammonia in its supercritical state.⁴⁸ However, these techniques are not practical for an industrial pretreatment method, as supercritical conditions and temperature fluctuations of those amplitudes often require high energy requirements. Therefore, we focused on working with ammonia under subcritical conditions, at set-point temperature and allowed it to contact cellulose for the desired shorter residence time.

The enzymatic hydrolysis results from **Fig. 2** show a progressive increase of hydrolysis yields as a function of increasing CIII crystallinity. Also, the results are consistent with our previous observation that higher CIII crystallinity favors improved enzymatic hydrolysis rates. Hydrolysis yields increased up to approximately two-fold from ~32% to ~ 59% for the most crystalline sample of CIII (i.e., 6:1) compared to native CI. This level of improvement has been observed previously by Chundawat et al. (2011)⁴⁸ using similar substrates and enzyme cocktails. However, in the literature it is possible to find a wider range of results. For example, Igarashi et al. (2007)¹³ observed even higher improvements when using purified enzymes to digest algae-derived CIII, resulting in approximately five folds higher glucose conversion when compared with algae-derived cellulose I. However, work by Chundawat et al. (2011 and 2013)^{3,14} and subsequent follow up studies by Shibafuji et al. (2014)⁴⁹ have shown that both enzyme cocktail composition and total enzyme loading can have a significant impact on CIII hydrolysis rates by fungal cellulases. On the other hand, Mittal et al. (2011)⁸ showed significantly lower improvements, or even no improvements after 24 h enzymatic hydrolysis of CIII compared with CI. Overall, differences in cellulose source, initial crystallinity, exact pretreatment method, cellulase cocktail composition, hydrolysis reaction time, and total enzyme loadings used in all these previous studies could explain some of the variability reported in the literature.

Effect of temperature and time on cellulose III formation: Temperature is another key factor contributing to CIII conversion as reported by several authors in the literature.^{8,19} This factor is not only important during evaporation of ammonia from the cellulose-ammonia complex, but also plays an important role during formation of the ammonia-cellulose intermediate.²⁶ Here, the temperature during ammonia evaporation was set constant at 25 °C. This temperature was controlled using absolute ethanol as the quenching or sampling solvent, which was placed in a

temperature-controlled water bath as described earlier. Ammonia was contacted with CI at temperatures at 25 °C or 90 °C to evaluate the effect of pretreatment temperature on the formation of crystalline CIII. These two temperatures are reasonably far apart from each other, allowing CIII conversion differences to be readily seen. Also, 90 °C was the maximum temperature limit observed for effective CIII conversion without thermally decomposing the sample. Maillard-based decomposition products derived from high temperature treatments (>100 °C) have been shown to inhibit enzymes during cellulose digestion (for Avicel PH-101)^{3,50} and therefore inadvertently impact the correlations drawn between hydrolysis yields and substrate crystallinity. This could explain some of the ambiguity in the correlations noted by Mittal et al. (2011) for CIII prepared from Avicel PH-101 at 130 °C for close to 60 mins.⁸

Residence time is also important for CIII conversion, as observed first by Clark et al. (1937)²¹ and Lewin et al. (1971).¹⁹ The latter observed a decrease in equatorial CrI with increasing time of ammonia treatment from 2 sec to 5 min. In that experiment, ammonia was evaporated from cotton samples that were dried at 105 °C. Lewin et al. (1971) also described the transition of CI to CIII as a function of treatment time, with increasing proportions of CIII for larger residence times. However, these authors did not quantify the relative proportions of total disordered cellulose (AC; based on lack of any significant equatorial reflections for (101), (10 $\bar{1}$), (002) crystallographic planes with well-defined XRD peaks at any Bragg angle), CI, and CIII content as a function of time using XRD and only allowed a maximum treatment time of 5 min. In Figure 3 it is possible to clearly observe the transition between these various crystalline allomorphs of cellulose as a function of treatment time. For this experiment, Avicel PH-101 was treated with 100% anhydrous liquid ammonia (6:1 ammonia-to-cellulose loading; dwb) at 25 °C and 90 °C in order to evaluate CIII conversion profiles at low versus high treatment temperatures, respectively. **Fig. 3** clearly shows an abrupt increase of CIII content within the first minute of contact of ammonia with cellulose quenched immediately after in ethanol, with CI rapidly depleted from the sample at 25 °C. This observation confirms that CIII can be formed at 25 °C with no further heating requirement. It also confirms the results obtained by Mittal et al. (2011), who observed complete CIII conversion at 25 °C for Avicel PH-101 and other sources of cellulose,⁸ including corn stover cellulose. **Fig. 3** also shows a rapid increase of the disordered or amorphous content of cellulose (AC) in the first minute of treatment, which slowly decreases with increasing pretreatment time. One possible explanation for this result is that ammonia could fully activate only some accessible regions of cellulose during the first minute of treatment, generating mainly CIII after ammonia removal from the ammonia-cellulose complex. As ammonia might not be able to rapidly access less exposed regions of the cellulose microfibrils and activate the ammonia-cellulose intermediate, these residual fiber regions could remain intact as native CI. However, even after the first minute of treatment, the AC content of the sample is continuing to drop till about 30 mins. This suggests that it might be also possible that there are some inherent kinetic limitations for cellulose chains restructuring or reannealing during formation of the ammonia-cellulose complex which is critical to the formation of highly ordered and crystalline CIII upon quenching of the complex in ethanol. The kinetics of the cellulose-ammonia complex reannealing will likely depend on the cellulose crystal size and degree of polymerization. Also, other accessible areas could be also partially activated by ammonia through the disruption of some hydrogen bonds, which during rapid ammonia evaporation might not align properly to generate a highly crystalline structure, resulting in a more amorphous CIII sample as suggested by XRD. Lewin et al. (1971)¹⁹ also showed an increase of the amorphous content of cotton in the first 5 min of treatment time. But since 5 mins

was the maximum residence time tested by Lewin, it might have not been long enough for ammonia to effectively penetrate the reactor packed with cotton fibers. Therefore, it was not possible for Lewin to observe the reduction of amorphous content once ammonia has completely penetrated inside the fibril to form a stable cellulose-ammonia complex prior to ammonia removal. Bellesia et al (2011) have used molecular dynamic simulations to analyze the initial interaction of CI with liquid ammonia.²⁶ This simulation study has shown how ammonia can rapidly penetrate into cellulose microfibrils and provided a theoretical basis for why the ammonia-cellulose complex is formed within a few seconds of contact of ammonia and cellulose. However, the simulation also indicates that there is relative shifting or reannealing of the cellulose layers within the fibril that in turn leads to the formation of channels that facilitate ammonia penetration into the fiber. This could explain why we have AC being produced in the initial penetration period when first contacting ammonia with cellulose.

At 90 °C, a similar CIII conversion profile could be observed, with a rapid increase of the amorphous content of cellulose, followed by its reduction for increasing treatment times. At the same time, a rapid increase of CIII conversion was observed as CI was depleted from the sample. However, a major difference between treatment at 25 °C and 90 °C is that at higher temperatures CIII is converted at a much faster rate, generating a sample of higher crystallinity than at lower temperatures. For example, the maximum amorphous content obtained at 90 °C was ~62%, while it was ~66% at 25 °C, both occurring only after 30 sec of treatment time. This result suggests that temperature plays an important role in promoting ammonia penetration into the cellulose fiber and formation of the ammonia-cellulose complex. This also supports previous simulation results obtained by Bellesia et al. (2011)²⁶ that clearly suggests an increase of ammonia penetration rate and cellulose-ammonia annealing with increasing treatment temperatures.

At 30 min residence time, the treated cellulose was totally depleted of CI and was composed mainly of disordered cellulose (or AC which is structurally not well-defined using XRD) and CIII at both 25 °C and 90 °C (Fig. 3). The main difference between the two samples at this time point was that at 90 °C, the sample contained approximately 49% of CIII, while at upon treatment at 25 °C the CIII content was only 41%. The effect of temperature during ammonia treatment of Avicel PH-101 was also reported by Mittal et al. (2011),⁸ with higher CrI observed for samples pretreated at higher temperatures. However, a comprehensive kinetics profile has never been reported in the literature showing the relative evolution of AC, CI, and CIII as a function of ammonia pretreatment time and temperature.

To evaluate the effect of pretreatment temperature and crystalline composition of cellulose on enzymatic hydrolysis rate, Avicel PH-101 was treated at three different temperatures (-30, 25, and 90 °C) for 30 minutes. Samples treated at 25 and 90 °C were quenched in ethanol at 25 °C prior to ammonia evaporation, while the sample treated at -30 °C was vacuum filtered and dried in the hood overnight at ambient temperature. The results presented here demonstrate that it is possible to obtain pretreated samples with significant variation in the levels of amorphous content for CIII. While at 25 and 90 °C it was possible to deplete the sample completely of native CI, fully being converted into CIII and/or AC, ammonia treatment performed at -30 °C generated a sample with poorly defined and highly amorphous-cellulose like XRD pattern that could not be completely deconvoluted and quantified as a mixture of AC, CI, and CIII. This XRD pattern suggests that ammonia treatment -30 °C promotes the formation of highly disordered cellulose with a much lower crystallinity index observed compared to CIII. Interestingly, this low temperature treated sample has a very broad equatorial reflection in the XRD spectra around the standard CIII (002)

crystallographic planes at approximately 20.6° Bragg angles (2θ). While, the lyophilized PASC sample gave a very broad equatorial reflection in the XRD spectra centered around 19.8° (2θ) with a very weak shoulder at 20.9° (2θ) as well. On a side note, the ammonia-cellulose complex samples quenched in water gave an XRD spectra in **Fig. 1** that was slightly distinct from the low temperature (-30 °C) treated sample with a very broad peak in the XRD spectra around 21.5° Bragg angles (2θ) that was clearly between the (002) crystallographic plane equatorial reflections expected for cellulose I or cellulose III. But much more detailed structural characterization would be needed to draw any conclusive inferences on the structural similarities/differences seen between these highly disordered cellulose samples. However, since it was challenging to glean any further structural information about the low temperature (-30 °C) treated sample using XRD alone, additional characterization was conducted using FT-Raman and FT-IR spectroscopy (see Fig. S2 and Fig. S7) as reported in the supplementary information (SI) section. FT-Raman spectrum of the -30 °C treated sample clearly contained spectral band features that were representative of cellulose-III based on peak assignments reported previously.^{51,52} For example, in the CCC/CCO/OCC/OCO skeletal bending vibrational energy region clear peaks were seen at 355, 425, and 463 cm⁻¹; in the CCC/CCO/COC/OCO bending and OH out-of-plane vibrational energy region clear peak was seen at 581 cm⁻¹; in the HCC/HCO bending at C6-hydroxymethyl position vibrational energy region clear peak was seen at 899 cm⁻¹; and finally in the CO/CC stretching vibrational energy region clear peak was seen at 899 cm⁻¹. However, additional peaks/shoulders unique to amorphous cellulose (i.e., lyophilized PASC) and/or native Avicel were also seen for the low-temperature treated sample alone (e.g., 309, 458, 519, 726, 1036, 1057, 1098, 1121, 1422 cm⁻¹). Also, unlike the 90 °C and 25 °C treated sample, the -30 °C treated sample clearly lacked sharp peaks and had broader shouldered peaks and the lowest intensity peaks in most cases. On the other hand, FT-IR had clear indication that the -30 °C treated sample had a much weaker shoulder peak at 3475 cm⁻¹ unlike higher temperature CIII samples, which is indicative of the weaker inter-molecular hydrogen bonding involving the hydroxymethyl group (O2-H...O6) in this sample. We also observed a marginally higher signal at 1640 cm⁻¹ in the FT-IR spectrum of the -30 °C treated sample compared to other crystalline allomorphs, suggesting a slightly higher capacity for free water to be associated with this form of disordered cellulose. Our XRD and spectroscopy analysis of the low temperature (-30 °C treated) ammonia treated samples suggest that this sample is composed of cellulose polymers arranged with some ultrastructural features that resemble crystalline CIII. However, the weakened FT-Raman spectral signals for the progressively lower temperature treatment samples suggests significant contribution from highly disordered amorphous cellulose. We hypothesize these increased AC content within ammonia treated samples to be intermediate transition states of the ammonia-cellulose complex that are thermally quenched and trapped at lower temperatures to prevent complete conversion of CI to CIII. Lastly, we haven't done any detailed structural analysis for the water quenched samples, so it is difficult to comment on the structural similarity of the disordered -30 °C treated versus the water quenched samples.

Similar effect of pretreatment temperature on CIII crystallinity was also observed by others, namely Saafan et al. (1984)⁵³ and Mittal et al. (2011).⁸ However, here we have much more precise control over the pretreatment conditions and can now systematically examine the impact of such structural modifications on enzymatic digestibility. The results presented in **Fig. 4** again support our previous observations that ammonia-treated cellulose samples with higher crystalline CIII content are more readily digestible by fungal cellulases. According to the predominantly accepted paradigm, cellulosic substrates containing higher amorphous content (as measured via

XRD) should be more digestible by cellulases.⁴³⁻⁴⁵ However, this is clearly in contradiction to our results presented in **Fig. 4** and elsewhere in this study. The existing paradigm is primarily based on results obtained using native cellulose (CI) and amorphous cellulose generated using ball milling or phosphoric acid treatments.^{36,54} From **Fig. 4** it is possible to clearly show that highly disordered cellulose created by ammonia treatment at -30 °C is more digestible than untreated Avicel (CI) composed by approximately 49.9 % of AC. However, PASC (composed of only AC), presents approximately 1.5-fold improvement with respect to the ammonia treated sample at -30 °C in hydrolysis rate. These observations suggest that different methods for creating AC generate quite distinct responses to enzymatic activity. Future work is required to better understand the basis for these differences at the structural level of cellulose, including evaluation of the level of cellulose hydrogen bonding, hydrophilicity, and enzyme accessible surface area. These studies also must be correlated with enzyme-substrate interaction measurements, such as binding affinity and catalytic activity of cellulases on the various amorphous substrates. A preliminary analysis of the apparent binding partition coefficient of a model GFP-labeled carbohydrate binding module (CBMs) to low (-30 °C treated) versus high (90 °C treated) CrI CIII samples clearly shows that the more disordered substrate is not as readily accessible to hydrolytic enzyme CBMs (see Fig. S3 in SI document). This could explain the poorer digestibility seen for the low (-30 °C treated) versus high (90 °C treated) CrI CIII samples. Furthermore, cellulose I also seems to have a higher apparent partition coefficient for the Type-A CBM than both cellulose III forms reported here. While this finding is consistent with previous reports of binding of Type-A CBM containing cellulases to cellulose III,^{3,14} we will be publishing additional papers to further explore the complex relationship between CBM binding versus cellulase activity on distinct cellulose allomorphs.

From the perspective of ammonia pretreatment of lignocellulosic biomass, it will likely be important to pretreat cellulose in order to obtain the highest possible content of highly crystalline CIII, which translates to a more efficient enzymatic digestion by fungal cellulases as shown by da Costa Sousa et al (2016).³² This work clearly shows that various levels of CIII, CI, and AC content can be achieved by controlling pretreatment variables such as temperature, reaction time, and ammonia loading.

Effect of ammonia-ethanol co-solvent concentration on cellulose III formation: CIII formation has been traditionally performed using ~100% anhydrous liquid ammonia pretreatment solvent loading, applying heat/pressure for relatively short periods of time (< 1h).¹⁹ As this method uses a liquefied gas, the pressure exerted while using ammonia alone can be considered a potential issue for economic and safety reasons. For example, when operating at 120 °C, pressure can increase up to approximately 1300 psi to maintain anhydrous ammonia in the liquid state (see Fig. S4 in SI). To avoid such high levels of operating pressure and to improve the economics and safety of the process, it would be important to test the usage of less volatile co-solvents, preferably polar solvents that allow formation of CIII, unlike water. As previously discussed, water does not allow CIII to be clearly formed without significant formation of highly disordered cellulose and therefore is not a viable option for this process. The current work confirmed ethanol as a compatible solvent to be used as a heat sink during ammonia evaporation. Ethanol and ammonia are also chemically compatible at temperatures below 150 °C, in the absence of other catalysts.^{55,56} Ultimately, ethanol is an inexpensive commodity chemical that is readily available, and is a major biofuel product produced by existing biorefineries. Therefore, this chemical could be considered a good candidate to be used as a co-solvent in an ammonia-based ‘organosolv-type’ pretreatment of lignocellulosic

biomass. Figure S4 shows the vapor-liquid equilibrium (VLE) curve of an ammonia-ethanol mixture at 120 °C. Upon analyzing this VLE data, it is evident that it would be possible to theoretically decrease the operating pressure below 750 psi for mixtures consisting of <60 wt% ammonia. However, it is important to evaluate the range of mass concentrations of ethanol-ammonia that would allow efficient CIII formation.

To determine the impact of co-solvent addition during pretreatment on CIII formation, Avicel PH-101 was pretreated with various concentrations of ammonia in a mixture of ammonia-ethanol, ranging from 17% to 60% ammonia (wt%), at different total added liquid-to-solid ratios, ranging from 4:1 to 10:1 (**Fig. 5**). These experiments were performed at 25 °C for 30 min residence time. The results show that both 17 and 33 wt% ammonia solutions are not concentrated enough to allow effective penetration of ammonia in the cellulose crystals and disrupt hydrogen bonding even at 10:1 liquid-to-solid loading. Since most of the native cellulose (CI) seems to present after pretreatment under such conditions it is likely that ethanol interferes with the initial formation of the ammonia-cellulose complex at 17 and 33 wt% ammonia concentration. However, using a 50 wt% ammonia solution, it was possible to observe some CIII conversion (21-27% based on XRD area), especially at 6:1 and 10:1 ammonia-to-cellulose ratios. At 4:1 there was a slightly lower CIII conversion compared to the latter two, which might have occurred due to mass action limitations. It is important to note that 4:1 liquid-to-solid ratio, using a 50 wt% ammonia solution, represents an effective 2:1 ammonia-to-cellulose ratio. From the results obtained in this experiment, CIII conversion could only be obtained after increasing the concentration of ammonia (in ethanol) from 33 wt% to 50 wt%. It is possible that ammonia concentration alone (i.e., law of mass action) is not responsible for the formation of the ammonia-cellulose complex intermediate in the presence of co-solvents like ethanol. For example, pH may also be responsible for improving solvation of the cellulose crystal by ammonia and perhaps facilitating the penetration of ammonia in the cellulose crystal. To probe such hypotheses, future studies are required where pH could be monitored and controlled during contact of CI with ammonia. When the concentration of ammonia was increased to 60 wt%, CIII conversion increased substantially for all liquid-to-solid ratios. As shown in **Fig. 5**, CIII conversion did not vary significantly within the range of liquid-to-solid ratios tested at 60 wt% ammonia. These results also show that about 5% of CI was still present in the various treated samples with 60 wt% ammonia. Nevertheless, it was possible to obtain approximately 40% of CIII and 55% of AC in all these samples. Also, unlike results shown in Figure 2 where cellulose was treated with ammonia for 10 minutes at 90 °C, increasing loadings of ammonia from 2:1 up to 6:1 resulted in a concomitant increase in the fraction of cellulose III formed. However, the experiments reported in figure 5 were performed at 25 °C for 30 min residence time and therefore, the results here may not be directly comparable to those reported in Fig. 2. In addition, liquid ammonia needs to fully submerge cellulose in order to promote cellulose III formation as it is well known that gaseous ammonia doesn't allow formation of cellulose III. This could potentially be challenging with the conditions close to 2:1-3:1 ammonia-to-cellulose loading since a small fraction of cellulose might not be fully immersed in liquid ammonia and that could explain the slightly lower conversion to cellulose III as observed in Fig 2. In the presence of a co-solvent like ethanol, it is likely that the cellulose sample is fully immersed in the pretreatment solvent at total liquid-to-solid loadings of 4:1 or higher (with 50% or higher ammonia in ethanol concentration). However, when using a solution of ammonia in ethanol or similar co-solvent, not only does the liquid-to-solid ratio become relevant to help promote cellulose III formation, or the effective ammonia-to-cellulose

ratio, but also the actual ammonia concentration in the co-solvent become critical as well (as seen in Fig. 5).

Figure 5 shows that at total liquid-to-solid ratios higher or equal to 4:1, the cellulose III formation was not impacted very significantly when we used the same 60% w/w concentration of ammonia in ethanol. However, in the case of 50% w/w ammonia-ethanol solution we see the % formation of cellulose III increases marginally at liquid-to-solid ratios greater than 4:1. Note that the density of the ethanol-ammonia pretreatment solution will also decrease with higher concentrations of ammonia in ethanol. Therefore, for the same liquid-to-solid ratio on a fixed mass basis, a solution of 60% ammonia will occupy a larger volume than a solution of 50% ammonia in ethanol. Therefore, 60% ammonia solution can likely fully submerge the biomass at slightly lower liquid-to-solid ratio than 50% ammonia solution. This may explain the differences seen in cellulose III formation profile between pretreatments performed using 50% ammonia versus 60% ammonia, in ethanol solution, as a function of various total liquid-to-solid ratios. In future work, it would be beneficial to clearly elucidate the role of biomass and ammonia-solvent specific density on cellulose III formation. Nevertheless, the main thing to point out from Fig. 5 is that a greater impact on cellulose III formation was observed when we increased the concentration of ammonia from 17% to 60% in ethanol at a fixed total liquid-to-solid loading. This clearly suggests that if we achieve a "saturation" point where the biomass is fully submerged, total liquid-to-solid ratio does not impact cellulose III formation very significantly. Instead, the kinetics of cellulose III formation may be more closely dependent on the concentration of ammonia in the co-solvent (i.e., ethanol) under those same loading conditions. However, detailed kinetic and structural studies will need to be performed in the future to better understand the role of concentration of polar co-solvents like ethanol on the formation as well as the stability of the cellulose-ammonia complex to eventually drive the formation of cellulose III during ammonia-based pretreatment of cellulosic biomass.

The enzymatic hydrolysis performance was also measured as a function of ammonia concentration and liquid-to-solid ratio, as presented in **Fig. 5**. These results show a trend comparable to findings reported in Fig. 1/2/3, where higher glucose yields tend to be achieved with increasing content of crystalline CIII in the treated sample. For the best condition tested herein, *i.e.* treatment with 60 wt% ammonia, our results show 55-57 % glucan conversion in the first 24h of enzymatic hydrolysis with 4 mg/g glucan of enzyme loading, independently of the liquid-to-solid ratio used. This result suggests that it is possible to achieve an increase of approximately 2-fold compared to untreated CI hydrolyzed under the same conditions (compare results with control in **Fig. 1**). At 4:1 liquid-to-solid ratio, the ammonia loading represents about 2.4 g/g of cellulose and an ethanol loading of 1.6 g/g of cellulose. In this specific study, the effect of temperature was not evaluated for the ammonia-ethanol system, since the major goal of this work was to determine the potential utilization of ethanol as a co-solvent to facilitate CIII formation (and possible extraction of lignin during application of a similar co-solvent based process for treating lignocellulosic biomass while also producing cellulose III). In this context, our results indicate that ethanol is a suitable co-solvent for such an application, generating a substrate enriched in CIII and allowing enzymatic hydrolysis results comparable to the ones obtained during a 10 min treatment using anhydrous ammonia alone at 25 °C. Also, the utilization of ethanol enables the possibility of operating at lower pressures during ammonia treatment, which could be a determining factor for the industrial implementation of an effective ammonia pretreatment technology based on CIII conversion of lignocellulosic biomass.

In summary, the key factors contributing to CIII conversion of Avicel PH-101 and its impact on enzymatic digestibility of cellulose were studied here. For this purpose, based on previous work,¹⁶ a modified hybrid methodology for XRD analysis consisting of the combination of amorphous subtraction and peak deconvolution methods was successfully implemented to determine relative amounts of crystalline CI, crystalline CIII, and disordered cellulose or AC. To better understand the impact of variables such as incubation temperature, ammonia loading, and residence time, it was also important to have constant temperature during ammonia removal after cellulose activation, which was revealed to be challenging due to heat of evaporation of ammonia. For this reason, another innovation was introduced in this work, consisting of the transfer of the ammonia-cellulose complex to ethanol solvent bath before ammonia was removed. This method allowed the ammonia evaporation at relatively stable temperatures avoiding inconsistent and misleading results. CIII conversion requires the access of liquid ammonia to the crystalline structure of cellulose and therefore, this process needed a minimum ratio of ammonia-to-cellulose to be effective. From our experiments, 3:1 was the minimum ammonia loading that could convert CI into CIII in the absence of co-solvents like ethanol. Higher ammonia loadings, such as 6:1, could improve CIII conversion by reducing the amorphous content of the treated sample. From pretreatment kinetics data using 6:1 ammonia-to-cellulose ratio, we could observe that CI is converted to different proportions of AC and CIII, depending on ammonia incubation time and temperature. In our experiments, the amorphous content of treated cellulose increased in the first few moments of ammonia impregnation. As time progressed, ammonia could incorporate more effectively into the crystalline structure of cellulose allowing a complete formation and annealing of the ammonia-cellulose complex, which was more efficiently converted to CIII after ammonia evaporation. This resulted in a decrease of the amorphous content of treated cellulose as a function of time. From enzymatic hydrolysis results, we concluded that higher crystalline CIII content benefits enzymatic hydrolysis rate, in contrast to some previous reports. Furthermore, the AC generated by very low-temperature based ammonia treatment cannot be compared with AC from PASC based on our combined XRD, FT-Raman, and FT-IR based analyses. Our work reiterates that not all amorphous cellulose sources are created equally and possibly have very distinct structural properties and recalcitrance towards hydrolytic cellulases. To maximize CIII conversion and reduce AC contents of treated samples it is important to use higher temperatures during treatment and longer residence times, with ammonia-to-cellulose mass ratios larger than 3:1. However, from the perspective of an ammonia-based pretreatment of lignocellulosic biomass, higher severity translates into additional processing costs. One of the most important processing issues when operating with ammonia at elevated temperatures is the operating pressure. To be able to decrease operating pressure while effectively converting CI to CIII and improving enzymatic hydrolysis yields, ammonia was used in solution with ethanol as co-solvent. In this final study, we observed that 60 wt% ammonia with ethanol as co-solvent allowed efficient conversion of CI to CIII at various liquid-to-solid ratios, while still enhancing enzymatic hydrolysis rates by 2-fold compared to untreated Avicel PH-101 similar to CIII substrate generated in the absence of any co-solvents.

Acknowledgements

SPSC also acknowledges support from the US National Science Foundation CBET, Rutgers University GAIA Award, and Oak Ridge Associated Universities (ORAU) Ralph E. Powe Junior Faculty Enhancement Award. We acknowledge support from the DOE Great

Lakes Bioenergy Research Center (DOE BER Office of Science DEFC02- 07ER64494). SPCS thanks Prof. Brian Fox (University of Wisconsin, Madison) for providing the GFP-CBM plasmid and Dr. Umesh Agarwal (Forest Products Laboratory, Madison) for providing access to the FT-Raman and FT-IR spectrometers. LDGS acknowledges Fundaçao para a Ciencia e a Tecnologia (QREN/POPH) grant number SFRH/BD/62517/2009. VB acknowledges the University of Houston High Priority Area Research Seed Grants and the State of Texas for startup funds.

Supporting Information (SI) File Description

See supplementary pdf document titled ‘Supplementary Information.pdf’ for supporting methods and results relevant to this study.

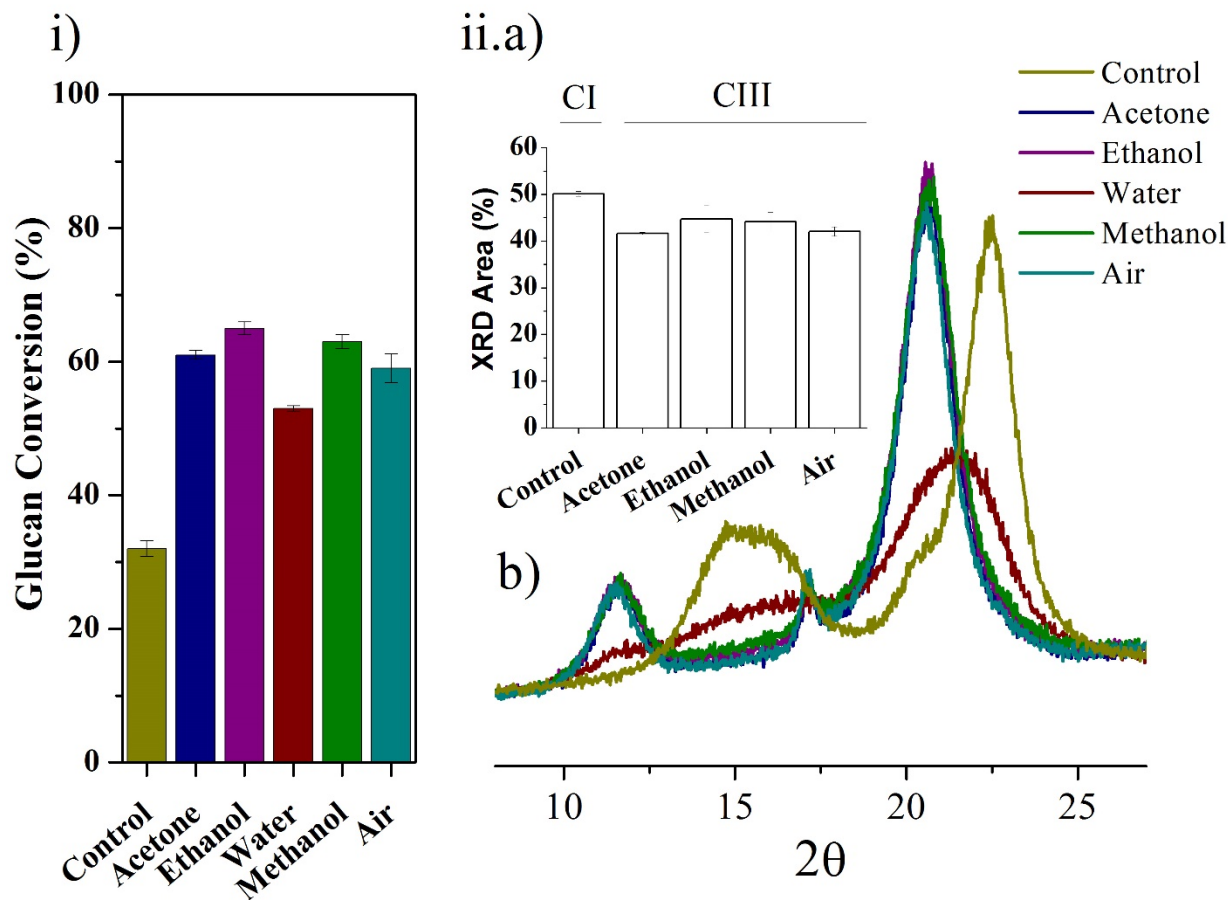


Figure 1. Effect of sampling or quenching solvent on cellulose III formation: Powder x-ray diffraction (XRD) spectra and enzymatic digestibility of Avicel PH-101 treated using liquid ammonia and the ammonia-cellulose complex then sampled or quenched in the presence of desired solvents (or directly in air) are shown here. (i) Glucan to glucose conversion yields during enzymatic hydrolysis of cellulosic substrates prepared by treatment at 90 °C with 6:1 (w/w) ammonia-to-cellulose ratio for 20 min residence time, sampled into various solvents or no solvent (air) are shown. The control experiment corresponds to native cellulose I (Avicel PH-101). Enzymatic digestions were all performed using 4 mg/g dry glucan enzyme loading of Accellerase 1500 for 24 h hydrolysis time. All hydrolysis assays were carried out in duplicate with mean values for glucan-to-glucose conversion reported here. Error bars shown indicate standard deviations ($\pm 1\sigma$) for reported mean values. (ii) Crystallinity index (CrI) of the various solvent quenched ammonia treated cellulose was calculated by the amorphous subtraction method as total crystalline cellulose XRD peak areas shown in a) based on original XRD spectra as shown in b). All XRD analyses were carried out in duplicate with mean values for total crystalline cellulose peak area reported here. Error bars shown indicate standard deviations ($\pm 1\sigma$) for reported mean values.

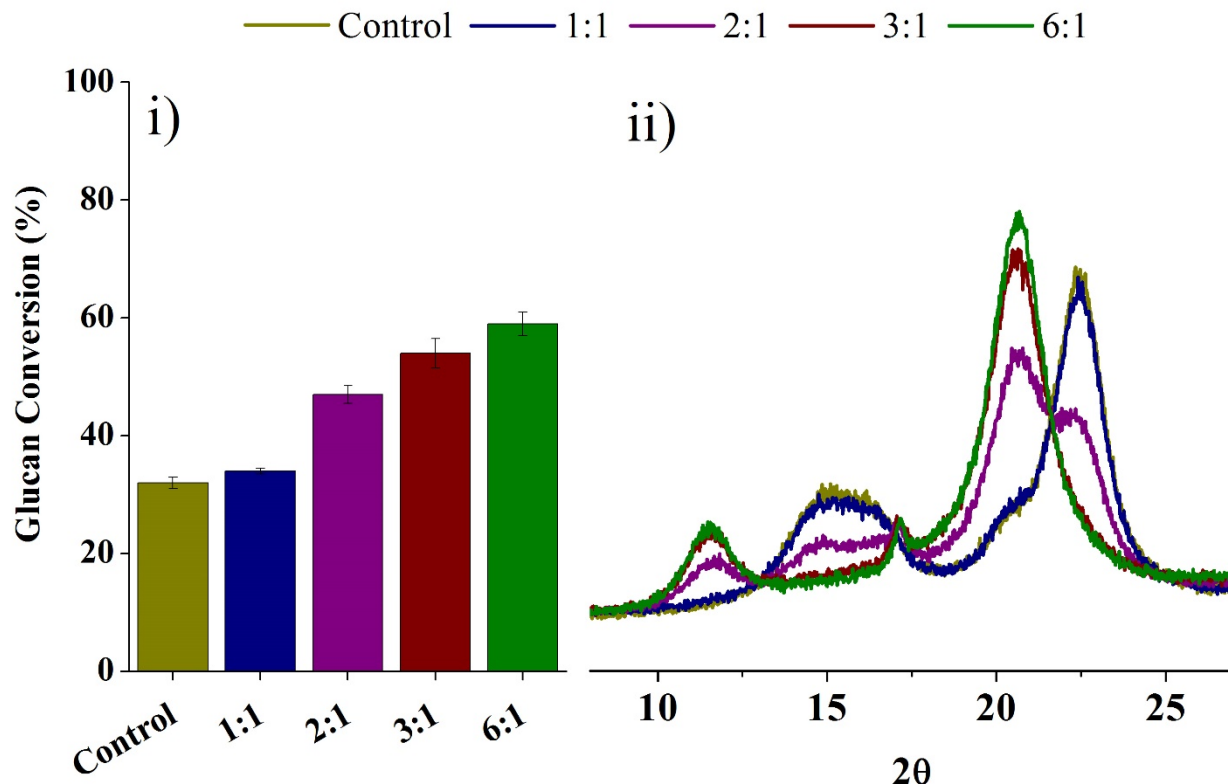


Figure 2. Effect of ammonia loading on cellulose III formation: Powder XRD spectra and enzymatic digestibility of Avicel PH-101 treated using various ammonia to cellulose mass ratios are shown here. (i) Glucan to glucose conversion yields during enzymatic hydrolysis of cellulosic substrates prepared by treatment under various ammonia:cellulose loading ratios, ranging from 1:1 to 6:1 (w/w; dwb), compared to the control (Avicel PH-101), are shown in the bar graph. Enzymatic digestions were all performed using 4 mg/g dry glucan enzyme loading of Accellerase 1500 for 24 h hydrolysis time. All hydrolysis assays were carried out in duplicate with mean values for glucan-to-glucose conversion reported here. Error bars shown indicate standard deviations ($\pm 1\sigma$) for reported mean values. ii) XRD spectra of ammonia treated cellulose prepared using various ammonia:cellulose ratios at 90 °C for 10 min residence time are shown here.

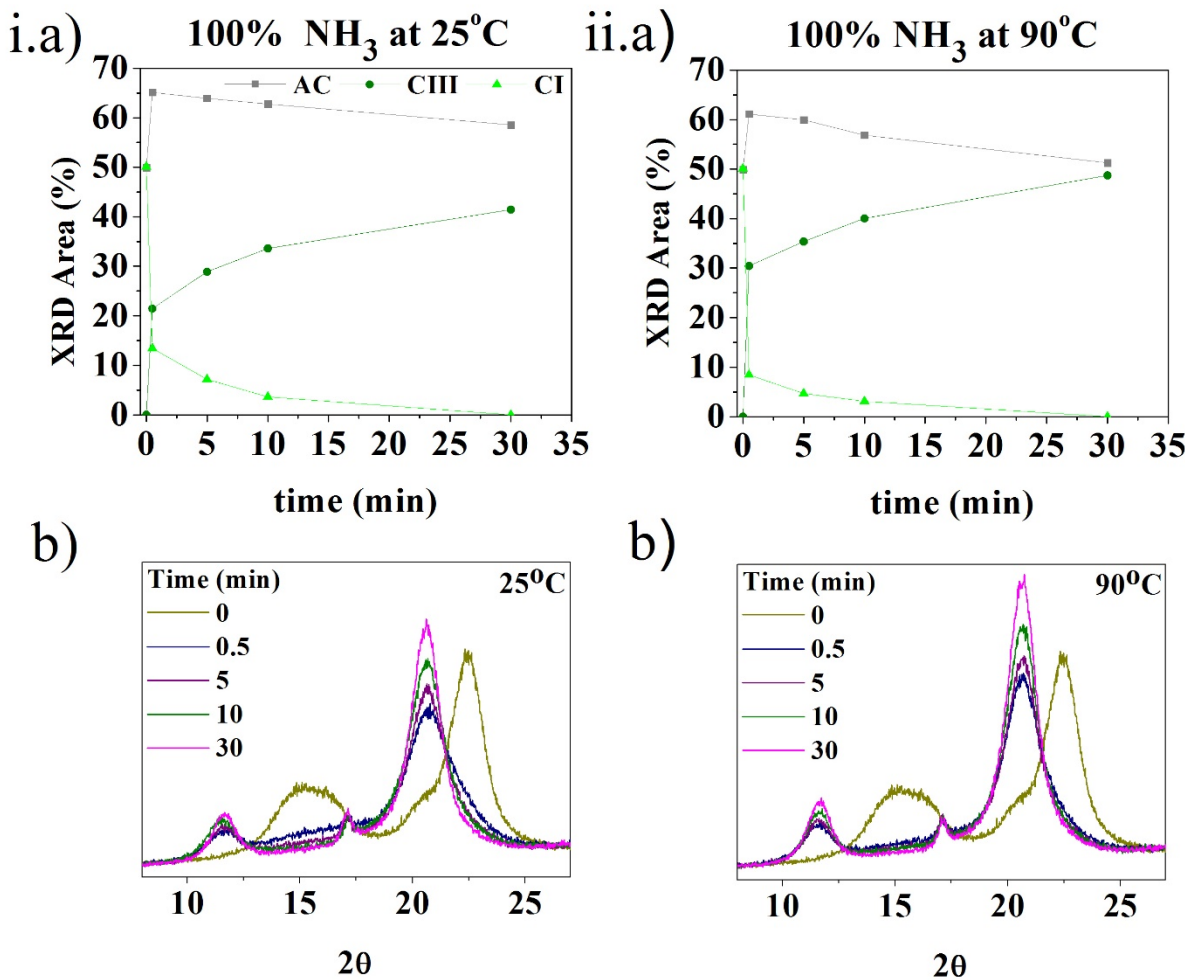


Figure 3. Effect of pretreatment temperature and time on cellulose III formation kinetics: Effect of CI to CIII conversion at low versus high pretreatment temperatures for varying residence times was studied using XRD. (i) Kinetic evolution of the relative proportions of cellulose III (CIII), cellulose I (CI), and disordered or amorphous cellulose (AC) during ammonia treatment of Avicel PH-101 at 25 °C as a function of residence time (a), and respective XRD spectra used to calculate CIII, CI, and AC contents at 25 °C (b) are shown here. (ii) Kinetic evolution of the relative proportions of cellulose III (CIII), cellulose I (CI) and amorphous cellulose (AC) during anhydrous ammonia treatment of Avicel PH-101 at 90 °C, as a function of residence time (a), and respective XRD spectra used to calculate CIII, CI, and AC contents at 90 °C are shown here. Crystallinity index (CrI) of the various ammonia treated cellulose was calculated by the amorphous subtraction method as total crystalline cellulose XRD peak areas shown in (a) insets based on original XRD spectra as shown in (b) insets. See Table S1 in SI document for XRD data replicates statistics for the final 30 min pretreated samples.

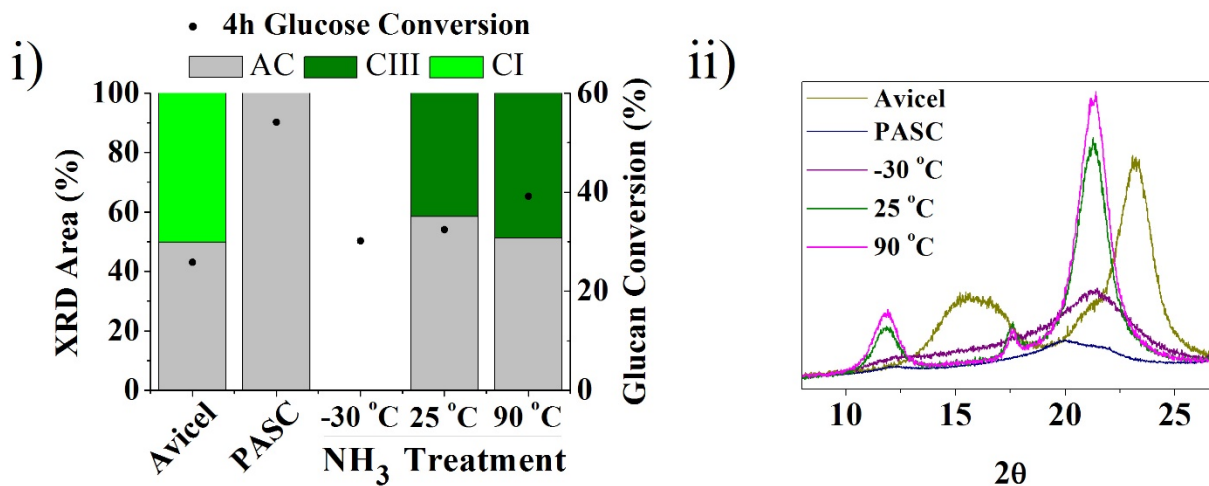


Figure 4. Effect of lower pretreatment temperatures on cellulose III formation and its enzymatic saccharification rate: Impact of pretreatment temperature on CIII crystallinity was studied to show that low XRD predicted sample crystallinity does not always correlate with improved enzymatic digestibility. (i) Comparison between amorphous content (left y-axis denoted as %contribution of AC, CIII, and CI to total XRD area in stacked bars) of Avicel PH-101 treated at various temperatures and correspondent effect on 4h glucose conversion (right y-axis denoted as %glucan-to-glucose hydrolysis yield denoted by filled circles) during enzymatic hydrolysis. Enzymatic hydrolysis was performed with 7.5 mg/g glucan of Accellerase 1500 enzymes at 50 °C. All hydrolysis assays were carried out in duplicate with mean values for glucan-to-glucose conversion reported here. Standard deviations ($\pm 1\sigma$) were always lower than 2% of the reported mean values, as shown in Table S1 of the SI document. (ii) XRD spectra of Avicel PH-101 treated with phosphoric acid (PASC) and with ammonia at -30, 25, and 90 °C. For 25 and 90 °C treatment, ammonia was evaporated at 25 °C after quenching the ammonia-cellulose complex in ethanol, while the -30 °C ammonia treated samples were vacuum filtered and dried in the hood at ambient temperatures.

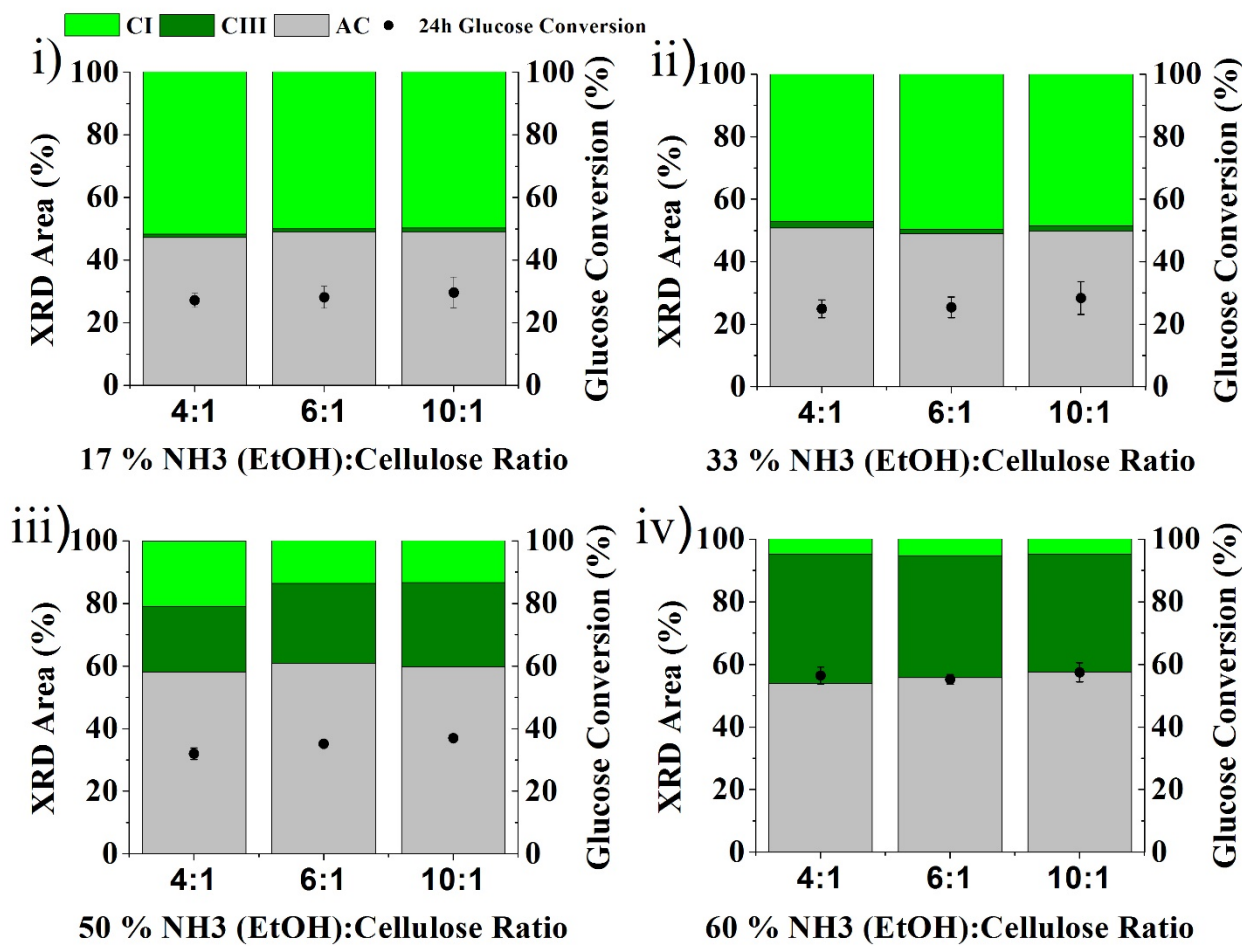
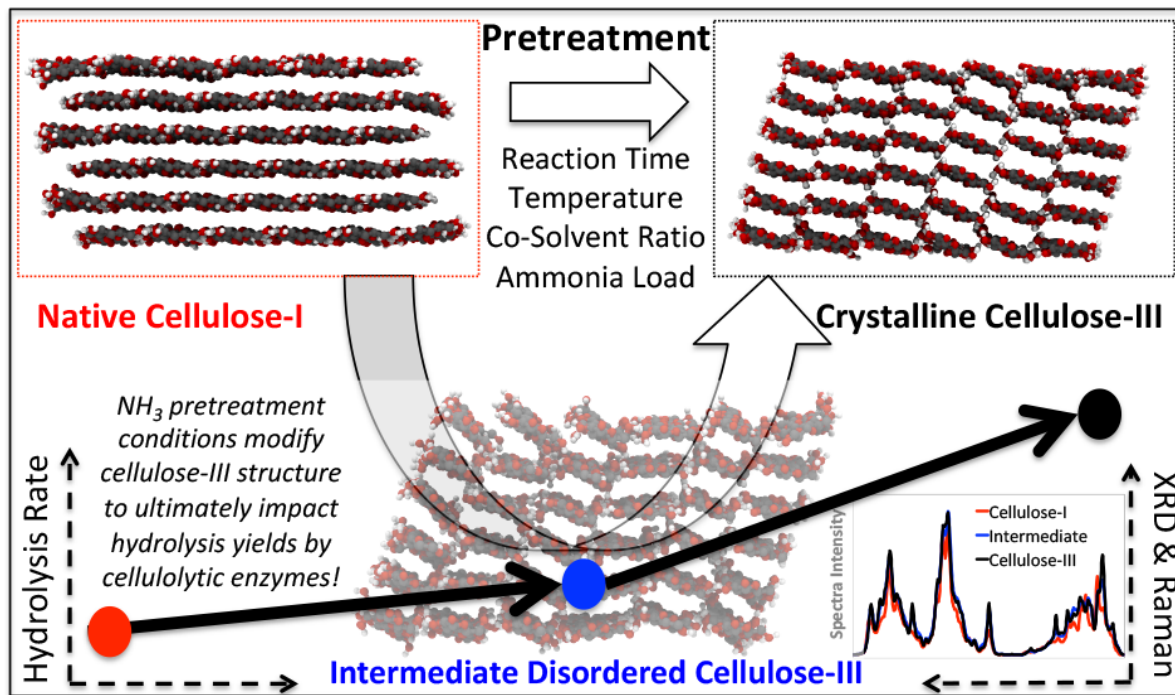


Figure 5. Effect of ammonia-ethanol concentration on cellulose III formation: Relative proportions (left y-axis denoted as %contribution of AC, CIII, and CI to total XRD area in stacked bars) of cellulose I (CI), cellulose III (CIII), and amorphous cellulose (AC) as a function of ammonia concentration (in ethanol) at various total added liquid-to-solid ratios during pretreatment and its impact on cellulose saccharification rate are shown here. Here, the ammonia concentrations (in ethanol) used in this study were 17 wt% (i), 33 wt% (ii), 50 wt% (iii) and 60 wt% (iv) for three fixed total added liquid-to-solid loadings. Ammonia treatment was performed at 25 °C for 30 min residence time using 4:1, 6:1, and 10:1 total added liquid-to-solid ratios for all ammonia (in ethanol) concentrations tested. The crystalline composition of cellulose was correlated with 24h glucose conversion (right y-axis denoted as %conversion denoted by filled circles) using 4 mg/g glucan loading of Accellerase 1500 for all samples. All hydrolysis assays were carried out in duplicate with mean values for glucan-to-glucose conversion reported here. Error bars shown indicate standard deviations ($\pm 1\sigma$) for reported mean values and cannot be seen sometimes if smaller than the symbol used here.

TOC/Abstract Graphic

TOC Synopsis: Ammonia-based pretreatment conditions can subtly change cellulose allomorphic ultrastructure to severely impact enzymatic hydrolysis rate



References

- (1) Beckham, G. T.; Matthews, J. F.; Peters, B.; Bomble, Y. J.; Himmel, M. E.; Crowley, M. F. Molecular-Level Origins of Biomass Recalcitrance: Decrystallization Free Energies for Four Common Cellulose Polymorphs. *J. Phys. Chem. B* **2011**, *115* (14), 4118–4127 DOI: 10.1021/jp1106394.
- (2) Weimer, P. J.; French, A. D.; Calamari Jr., T. A. Differential Fermentation of Cellulose Allomorphs by Ruminal Cellulolytic Bacteria. *Appl. Environ. Microbiol.* **1991**, *57* (11), 3101–3106.
- (3) Chundawat, S. P. S.; Bellesia, G.; Uppugundla, N.; Sousa, L.; Gao, D.; Cheh, A.; Agarwal, U.; Bianchetti, C.; Phillips, G.; Langan, P.; Balan, V.; Gnanakaran, S.; Dale, B. E. Restructuring the Crystalline Cellulose Hydrogen Bond Network Enhances Its Depolymerization Rate. *J. Am. Chem. Soc.* **2011**, *133* (29), 11163–11174 DOI: 10.1021/ja2011115.
- (4) Hall, M.; Bansal, P.; Lee, J. H.; Realff, M. J.; Bommarius, A. S. Cellulose Crystallinity - a Key Predictor of the Enzymatic Hydrolysis Rate. *FEBS J.* **2010**, *277* (6), 1571–1582.
- (5) Nishiyama, Y.; Sugiyama, J.; Chanzy, H.; Langan, P. Crystal Structure and Hydrogen Bonding System in Cellulose Ia. *J. Amer. Chem. Soc.* **2003**, *125*, 14300–14306.
- (6) Nishiyama, Y.; Langan, P.; Chanzy, H. Crystal Structure and Hydrogen-Bonding System in Cellulose Ib from Synchrotron X-Ray and Neutron Fiber Diffraction. *J. Am. Chem. Soc.* **2002**, *124* (31), 9074–9082 DOI: 10.1021/ja0257319.
- (7) Igarashi, K.; Wada, M.; Samejima, M. Activation of Crystalline Cellulose to Cellulose III Results in Efficient Hydrolysis by Cellobiohydrolase. *FEBS J.* **2007**, *274* (7), 1785–1792 DOI: 10.1111/j.1742-4658.2007.05727.x.
- (8) Mittal, A.; Katahira, R.; Himmel, M.; Johnson, D. Effects of Alkaline or Liquid-Ammonia Treatment on Crystalline Cellulose: Changes in Crystalline Structure and Effects on Enzymatic Digestibility. *Biotechnol. Biofuels* **2011**, *4* (1), 41.
- (9) Chundawat, S. P. S.; Paavola, C. D.; Raman, B.; Nouailler, M.; Chan, S. L.; Mielenz, J. R.; Brechot, V. R.; Trent, J. D.; Dale, B. E. Saccharification of Thermochemically Pretreated Cellulosic Biomass Using Native and Engineered Cellulosomal Enzyme Systems. *React. Chem. Eng.* **2016**, *1* (6), 616–628 DOI: 10.1039/c6re00172f.
- (10) Weimer, P. J.; Lopez-Guisa, J. M.; French, A. D. Effect of Cellulose Fine Structure on Kinetics of Its Digestion by Mixed Ruminal Microorganisms in Vitro. *Appl. Environ. Microbiol.* **1990**, *56* (8), 2421–2429.
- (11) Cui, T.; Li, J.; Yan, Z.; Yu, M.; Li, S. The Correlation between the Enzymatic Saccharification and the Multidimensional Structure of Cellulose Changed by Different Pretreatments. *Biotechnol. Biofuels* **2014**, *7* (1), 134 DOI: 10.1186/s13068-014-0134-6.
- (12) Wada, M.; Ike, M.; Tokuyasu, K. Enzymatic Hydrolysis of Cellulose I Is Greatly Accelerated via Its Conversion to the Cellulose II Hydrate Form. *Polym. Degrad. Stab.* **2010**, *95* (4), 543–548.
- (13) Igarashi, K.; Wada, M.; Samejima, M. Activation of Crystalline Cellulose to Cellulose III Results in Efficient Hydrolysis by Cellobiohydrolase. *FEBS J.* **2007**, *274* (7), 1785–1792 DOI: 10.1111/j.1742-4658.2007.05727.x.
- (14) Gao, D.; Chundawat, S. P. S.; Sethi, A.; Balan, V.; Gnanakaran, S.; Dale, B. E. Increased Enzyme Binding to Substrate Is Not Necessary for More Efficient Cellulose Hydrolysis. *Proc. Natl. Acad. Sci.* **2013**, *110* (27), 10922–10927 DOI: 10.1073/pnas.1213426110.

(15) Brady, S. K.; Sreelatha, S.; Feng, Y.; Chundawat, S. P. S.; Lang, M. J. Cellobiohydrolase 1 from *Trichoderma Reesei* Degrades Cellulose in Single Cellobiose Steps. *Nat. Commun.* **2015**, *6*, 10149 DOI: 10.1038/ncomms10149.

(16) Park, S.; Baker, J.; Himmel, M.; Parilla, P.; Johnson, D. Cellulose Crystallinity Index: Measurement Techniques and Their Impact on Interpreting Cellulase Performance. *Biotechnol. Biofuels* **2010**, *3* (1), 10.

(17) Schleicher, H.; Daniels, C.; Philipp, B. Changes of Cellulose Accessibility to Reactions in Alkaline Medium by Activation with Ammonia. *J. Polym. Sci. Part C-Polymer Symp.* **1974**, No. 47, 251–260.

(18) Barry, A. J.; Peterson, F. C.; King, A. J. X-Ray Studies of Reactions of Cellulose in Non-Aqueous Systems. I. Interaction of Cellulose and Liquid Ammonia. *J. Am. Chem. Soc.* **1936**, *58* (2), 333–337.

(19) Lewin, M.; Roldan, L. G. The Effect of Liquid Anhydrous Ammonia in the Structure and Morphology of Cotton Cellulose. *J. Polym. Sci. Part C-Polymer Symp.* **1971**, No. 36, 213–229.

(20) Davis, W. E.; Barry, A. J.; Peterson, F. C.; King, A. J. X-Ray Studies of Reactions of Cellulose in Non-Aqueous Systems. II. Interaction of Cellulose and Primary Amines. *J. Am. Chem. Soc.* **1943**, *65* (7), 1294–1299 DOI: 10.1021/ja01247a012.

(21) Clark, G. L.; Parker, E. A. An X-Ray Diffraction Study of the Action of Liquid Ammonia on Cellulose and Its Derivatives. *J. Phys. Chem.* **1937**, *41* (6), 777–786 DOI: 10.1021/j150384a001.

(22) Chundawat, S. P. S.; Bals, B.; Campbell, T.; Sousa, L.; Gao, D.; Jin, M.; Eranki, P.; Garlock, R.; Teymouri, F.; Balan, V.; Dale, B. E. Primer on Ammonia Fiber Expansion Pretreatment. In *Aqueous Pretreatment of Plant Biomass for Biological and Chemical Conversion to Fuels and Chemicals*; John Wiley & Sons, Ltd, 2013; pp 169–200.

(23) Hess, K.; Gundermann, J. The Effect of Liquid Ammonia on Cellulose Fibers (Formation from Ammonia-Cellulose I, Ammonia-Gellulose II and Cellulose III). *Berichte Der Dtsch. Chem. Gesellschaft* **1937**, *70*, 1788–1799.

(24) Yatsu, L. Y.; Calamari, T. A.; Benerito, R. R. Conversion of Cellulose I to Stable Cellulose III. *Text. Res. J.* **1986**, *56* (7), 419–424 DOI: 10.1177/004051758605600704.

(25) Bellesia, G.; Chundawat, S. P. S.; Langan, P.; Redondo, A.; Dale, B. E.; Gnanakaran, S. Coarse-Grained Model for the Interconversion between Native and Liquid Ammonia-Treated Crystalline Cellulose. *J. Phys. Chem. B* **2012**, *116* (28), 8031–8037 DOI: 10.1021/jp300354q.

(26) Bellesia, G.; Chundawat, S. P. S.; Langan, P.; Dale, B. E.; Gnanakaran, S. Probing the Early Events Associated with Liquid Ammonia Pretreatment of Native Crystalline Cellulose. *J. Phys. Chem. B* **2011**, *115* (32), 9782–9788 DOI: 10.1021/jp2048844.

(27) Wada, M.; Nishiyama, Y.; Bellesia, G.; Forsyth, T.; Gnanakaran, S.; Langan, P. Neutron Crystallographic and Molecular Dynamics Studies of the Structure of Ammonia-Cellulose I: Rearrangement of Hydrogen Bonding during the Treatment of Cellulose with Ammonia. *Cellulose* **2011**, *18* (2), 191–206 DOI: 10.1007/s10570-010-9488-5.

(28) Cuculo, J. A.; Smith, C. B.; Sangwatanaroj, U.; Stejskal, E. O.; Sankar, S. S. A Study on the Mechanism of Dissolution of the Cellulose/NH₃/NH₄SCN System. II. *J. Polym. Sci. Part A Polym. Chem.* **1994**, *32* (2), 241–247.

(29) Cuculo, J. A.; Smith, C. B.; Sangwatanaroj, U.; Stejskal, E. O.; Sankar, S. S. A Study on

the Mechanism of Dissolution of the Cellulose/NH₃/NH₄SCN System. *I. J. Polym. Sci. Part A Polym. Chem.* **1994**, *32* (2), 229–239.

(30) Weimer, P. J.; Chou, Y. C. T.; Weston, W. M.; Chase, D. B. Effect of Supercritical Ammonia on the Physical and Chemical Structure of Ground Wood. *Biotechnol Bioeng Symp* **1986**, *17*, 5–18.

(31) Jin, M.; da Costa Sousa, L.; Schwartz, C.; He, Y.; Sarks, C.; Gunawan, C.; Balan, V.; Dale, B. E. Toward Lower Cost Cellulosic Biofuel Production Using Ammonia Based Pretreatment Technologies. *Green Chem.* **2016**, *18* (4), 957–966 DOI: 10.1039/C5GC02433A.

(32) da Costa Sousa, L.; Jin, M.; Chundawat, S. P. S.; Bokade, V.; Tang, X.; Azarpira, A.; Lu, F.; Avci, U.; Humpula, J.; Uppugundla, N.; Gunawan, C.; Pattathil, S.; Cheh, A. M.; Kothari, N.; Kumar, R.; Ralph, J.; Hahn, M. G.; Wyman, C. E.; Singh, S.; Simmons, B. A.; Dale, B. E.; Balan, V. Next-Generation Ammonia Pretreatment Enhances Cellulosic Biofuel Production. *Energy Environ. Sci.* **2016**, *9*, 1215–1223 DOI: 10.1039/C5EE03051J.

(33) Ruland, W. X-Ray Determination of Crystallinity and Diffuse Disorder Scattering. *Acta Cryst* **1961**, *14*, 1180–1185.

(34) Garvey, C. J.; Parker, I. H.; Simon, G. P. On the Interpretation of X-Ray Diffraction Powder Patterns in Terms of the Nanostructure of Cellulose I Fibres. *Macromol. Chem. Phys.* **2005**, *206* (15), 1568–1575 DOI: 10.1002/macp.200500008.

(35) Chundawat, S. P. S.; Vismeh, R.; Sharma, L. N.; Humpula, J. F.; da Costa Sousa, L.; Chambliss, C. K.; Jones, A. D.; Balan, V.; Dale, B. E. Multifaceted Characterization of Cell Wall Decomposition Products Formed during Ammonia Fiber Expansion (AFEX) and Dilute-Acid Based Pretreatments. *Bioresour. Technol.* **2010**, *101*, 8429–8438 DOI: 10.1016/j.biortech.2010.06.027.

(36) Zhang, Y. H. P.; Cui, J. B.; Lynd, L. R.; Kuang, L. R. A Transition from Cellulose Swelling to Cellulose Dissolution by O-Phosphoric Acid: Evidence from Enzymatic Hydrolysis and Supramolecular Structure. *Biomacromolecules* **2006**, *7*, 644–648.

(37) Walseth, C. S. Occurrence of Cellulase in Enzyme Preparations from Microorganisms. *Tappi* **1952**, *35*, 228–233.

(38) Resch, M. G.; Baker, J. O.; Decker, S. R. Low Solids Enzymatic Saccharification of Lignocellulosic Biomass. *Tech. Rep. NREL/TP-5100-63351, Lab. Anal. Proced.* **2015**, No. February, 1–9 DOI: 10.1016/j.jallcom.2018.03.019.

(39) Chundawat, S. P. S.; Lipton, M. S.; Purvine, S. O.; Uppugundla, N.; Gao, D.; Balan, V.; Dale, B. E. Proteomics Based Compositional Analysis of Complex Cellulase-Hemicellulase Mixtures. *J. Proteome Res.* **2011**, *10* (10), 4365–4372 DOI: 10.1021/pr101234z.

(40) Schuerch, C. Plasticizing Wood with Liquid Ammonia. *J. Ind. Eng. Chem.* **1963**, *55*, 39.

(41) Wada, M.; Nishiyama, Y.; Langan, P. X-Ray Structure of Ammonia-Cellulose I: New Insights into the Conversion of Cellulose I to Cellulose III. *Macromolecules* **2006**, *39* (8), 2947–2952 DOI: 10.1021/ma060228s.

(42) Thygesen, A.; Oddershede, J.; Lilholt, H.; Thomsen, A. B.; Ståhl, K. On the Determination of Crystallinity and Cellulose Content in Plant Fibres. *Cellulose* **2005**, *12* (6), 563–576.

(43) Hall, M.; Bansal, P.; Lee, J. H.; Realff, M. J.; Bommarius, A. S. Cellulose Crystallinity – a Key Predictor of the Enzymatic Hydrolysis Rate. *FEBS J.* **2010**, *277* (6), 1571–1582 DOI: 10.1111/j.1742-4658.2010.07585.x.

(44) Sinitsyn, A.; Gusakov, A.; Vlasenko, E. Effect of Structural and Physico-Chemical Features

of Cellulosic Substrates on the Efficiency of Enzymatic Hydrolysis. *Appl Biochem Biotechnol* **1991**, *30*, 43–59.

(45) Gharpuray, M. M.; Lee, Y.; Fan, L. T. Structural Modification of Lignocellulosics by Pretreatments to Enhance Enzymatic Hydrolysis. *Biotechnol Bioeng* **1983**, *25*, 157–172.

(46) Murnen, H. K.; Balan, V.; Chundawat, S. P. S.; Bals, B.; Sousa, L. D.; Dale, B. E. Optimization of Ammonia Fiber Expansion (AFEX) Pretreatment and Enzymatic Hydrolysis of Miscanthus x Giganteus to Fermentable Sugars. *Biotechnol. Prog.* **2007**, *23* (4), 846–850 DOI: 10.1021/bp070098m.

(47) Balan, V.; Bals, B.; Chundawat, S. P.; Marshall, D.; Dale, B. E. Lignocellulosic Biomass Pretreatment Using AFEX. In *Biofuels: Methods and Protocols*; 2009; Vol. 581, pp 61–77.

(48) Wada, M.; Heux, L.; Isogai, A.; Nishiyama, Y.; Chanzy, H.; Sugiyama, J. Improved Structural Data of Cellulose III Prepared in Supercritical Ammonia. *Macromolecules* **2001**, *34* (5), 1237–1243.

(49) Shibafuji, Y.; Nakamura, A.; Uchihashi, T.; Sugimoto, N.; Fukuda, S.; Watanabe, H.; Samejima, M.; Ando, T.; Noji, H.; Koivula, A.; Igarashi, K.; Iino, R. Single-Molecule Imaging Analysis of Elementary Reaction Steps of Trichoderma Reesei Cellobiohydrolase I (Cel7A) Hydrolyzing Crystalline Cellulose I α and III. *J. Biol. Chem.* **2014**, *289*, 14056–14065 DOI: 10.1074/jbc.M113.546085.

(50) Humpula, J. F.; Uppugundla, N.; Vismeh, R.; Sousa, L.; Chundawat, S. P. S.; Jones, A. D.; Balan, V.; Dale, B. E.; Cheh, A. M. Probing the Nature of AFEX-Pretreated Corn Stover Derived Decomposition Products That Inhibit Cellulase Activity. *Bioresour. Technol.* **2014**, *152*, 38–45 DOI: 10.1016/j.biortech.2013.10.082.

(51) Agarwal, U. P. 1064 Nm FT-Raman Spectroscopy for Investigations of Plant Cell Walls and Other Biomass Materials. *Front. Plant Sci.* **2014**, *5*, 490 DOI: 10.3389/fpls.2014.00490.

(52) Agarwal, U.; Reiner, R.; Ralph, S. Cellulose I Crystallinity Determination Using FT-Raman Spectroscopy: Univariate and Multivariate Methods. *Cellulose* **2010**, *17* (4), 721–733.

(53) Saafan, A. A.; Kandil, S. H.; Habib, A. M. Liquid-Ammonia and Caustic Mercerization of Cotton Fibers Using X-Ray, Infrared, and Sorption Measurements. *Text Res J* **1984**, *54*, 863–867.

(54) Wadehra, I. L.; Manley, R. S. J.; Goring, D. A. I. Permanently Amorphous Cellulose. *J. Appl. Polym. Sci.* **1965**, *9* (7), 2634–2636 DOI: 10.1002/app.1965.070090725.

(55) Bel'chev, F. V; Shuikin, N. I.; Novikov, S. S. The Catalytic Amination of Alcohols. *Bull. Acad. Sci. USSR, Div. Chem. Sci.* **1961**, *10* (4), 599–602 DOI: 10.1007/bf00909128.

(56) Klinkenberg, J. L.; Hartwig, J. F. Catalytic Organometallic Reactions of Ammonia. *Angew. Chemie Int. Ed.* **2010**, *50* (1), 86–95 DOI: 10.1002/anie.201002354.

Supporting Information (SI) Document:

Impact of ammonia pretreatment conditions on cellulose III allomorph ultrastructure and its enzymatic digestibility

Leonardo da Costa Sousa^{1*}, James Humpula¹, Venkatesh Balan²,
Bruce E. Dale¹, Shishir P.S. Chundawat^{3*}

¹ DOE Great Lakes Bioenergy Research Center (GLBRC), Department of Chemical Engineering and Materials Science, Michigan State University, Lansing, MI 48910, USA

² Department of Engineering Technology, College of Technology, Biotechnology Program, University of Houston, 304A College of Technology Building, Houston, TX, 77204, USA

³ Department of Chemical and Biochemical Engineering, Rutgers State University of New Jersey, 98 Brett Road, Piscataway, NJ, 08854, USA

Number of Pages: 16

Number of Figures: 7

Number of Tables: 1

* Corresponding Authors:

Shishir P.S. Chundawat (Email: shishir.chundawat@rutgers.edu; Phone: +1-848-445-3678); Department of Chemical and Biochemical Engineering, Rutgers, The State University of New Jersey, 98 Brett Road, Engineering Building Room C150A, Piscataway, NJ, 08854, USA) and Leonardo da Costa Sousa (Email: sousaleo80@gmail.com) DOE Great Lakes Bioenergy Research Center (GLBRC), Department of Chemical Engineering and Materials Science, Michigan State University, 3815 Technology Boulevard, Lansing, MI 48910, USA.

Supporting Experimental Methods Section:

M1. Effect of ammonia-cellulose complex sampling or quenching solvent on CIII formation

The ammonia-cellulose complex was first produced using a high pressure reaction vessel and contacting anhydrous liquid ammonia with Avicel PH-101 (Sigma-Aldrich, St.Louis, MO, USA) at a 6:1 ammonia-to-cellulose ratio (dwb), at 90 °C for 20 min total residence time. The reaction occurred under 1000 psi of nitrogen overpressure to assure all the loaded ammonia was in the liquid phase. Next, suspensions of ammonia-cellulose complex in liquid ammonia were sampled directly through the reactor dip tube into a vessel containing excess of desired quenching/sampling solvents at 25 °C. These vessels were kept in a room temperature-controlled water bath to prevent temperature drop during ammonia evaporation. The quenching/sampling solvents used in this study were acetone, methanol, ethanol and water, in a proportion of approximately 30:1 (v/v) solvent-to-sampled volume. Ammonia pressure was released from the top of the sampling vessel and the resulting cellulose fibers solvent suspension were then filtered using a Millipore (Billerica, MA, USA) vacuum-filtration system equipped with a glass microfiber filter (Whatman GF/A, Kent, UK). The treated cellulose samples were further washed with the respective solvents and dried overnight in the fume hood to evaporate residual solvent. Samples were stored in zip sealed plastic bags at 4°C prior to usage. XRD was performed in these treated samples within the first 48 h after reaction completion.

M2. Effect of ammonia to cellulose loading on CIII formation

The ammonia-cellulose complex was formed using various loadings of anhydrous ammonia, notably 1:1, 2:1, 3:1 and 6:1 ammonia-to-cellulose ratio (dwb), at 90 °C for 10 min residence time. The microcrystalline cellulose used in this study was Avicel PH-101 (Sigma-Aldrich, St. Louis, MO, USA). The ammonia-cellulose complex activation occurred under 1000 psi of nitrogen overpressure to assure all the loaded ammonia was in the liquid phase. A suspension of that intermediate complex was then transferred to 100% ethanol quenching/sampling solvent in a ratio of approximately 30:1 solvent-to-sample, which was maintained at 25 °C in a temperature-controlled water bath. Ammonia pressure was released from the top of the sampling vessel and the resulting cellulose fibers were filtered using a Millipore (Billerica, MA, USA) vacuum-filtration system equipped with a glass microfiber filter (Whatman GF/A, Kent, UK). The treated cellulose samples were further washed with absolute ethanol and dried overnight in the hood to evaporate residual solvent. Samples were stored in zip sealed plastic bags at 4 °C prior to usage. XRD was performed in these treated samples within the first 48 h after reaction completion.

M3. Effect of pretreatment temperature and time on CIII conversion

In these experiments, ammonia was added to a high-pressure reaction vessel containing Avicel PH-101 at set point temperature, using a syringe pump (Teledyne Isco Model 500D, Lincoln, NK, USA). Ammonia-cellulose complexes were formed solely with anhydrous ammonia, using 6:1 ammonia-to-cellulose ratio (dwb), at various temperatures (ranging from -30 °C to 90 °C). All incubations were performed for 30 min total residence time and 1000 psi of nitrogen overpressure to assure that all added ammonia was in liquid state and in contact with cellulose. In this study, it was important to differentiate between the effects of temperature during ammonia-cellulose complex formation and temperature of CIII conversion during ammonia evaporation. For this purpose, ammonia-cellulose complexes formed at the various temperatures were sampled to a vessel containing excess of 100% ethanol at a constant temperature of 25 °C. The cellulose

suspensions in ethanol, obtained after ammonia evaporation from the sampling vessel, were further filtered using a Millipore (Billerica, MA, USA) vacuum-filtration system equipped with a glass microfiber filter (Whatman GF/A, Kent, UK). Residual ammonia was further removed by flowing 100% ethanol through the sample while applying vacuum to the filtration system. Ammonia-treated cellulose samples were further dried in the hood overnight to evaporate residual ethanol. Samples were stored in zip sealed plastic bags at 4 °C prior to usage. XRD was performed in these treated samples within the first 48 h after reaction completion.

M4. Effect of ethanol:ammonia co-solvent concentration on CIII conversion

Avicel PH-101 was placed in the high-pressure reactor in the presence of calculated amounts of 100% ethanol. Appropriate volumes of ammonia were then loaded into the reactor with a syringe pump at 25 °C. Several concentrations of ammonia in ethanol were tested, ranging from 17 wt% to 60 wt% ammonia. Liquid-to-solid ratios were also varied for a fixed ammonia-to-cellulose concentration, ranging from 4:1 to 10:1 (w/w; dwb). Avicel PH-101 was incubated in these ammonia solutions at 25 °C for 30 min residence time before being transferred through a sampling valve to a vessel containing absolute ethanol at 25 °C. Ammonia was further evaporated from the sampling vessel and the cellulose suspension was transferred to a vacuum filtration system (EMD Millipore, Billerica, MA, USA), equipped with glass microfiber filters (Whatman GF/A, Kent, UK). The treated cellulose was extensively washed with 100% ethanol to remove residual ammonia. Treated cellulose samples were air dried overnight in the hood to evaporate residual ethanol prior to storage in zip sealed plastic bags at 4 °C. XRD was performed in these treated samples within the first 48 hours after reaction completion.

M5. XRD method and data analysis to estimate crystallinity index

XRD was performed on an X-ray powder diffractometer with beam parallelized by a Gobel mirror (D8 Advance with Lynxeye detector; Bruker, Bruker AXS Inc., Madison, WI, USA). CuK α radiation (wavelength = 1.5418 Å) was generated at 40 kV and 40 mA. Detector slit was set to 2.000 mm. Sample was analyzed using a coupled 20/θ scan type with a continuous PSD fast scan mode. 20 started at 8.000° and ended at 30.0277° with increments of 0.02151°, while θ started at 4.0000° and ended at 15.0138° with increments of 0.01075°. Step time was 1.000 sec (i.e., 1025 total steps, effective total time 1157 sec per run). Lyophilized cellulose samples (approximately 0.5 g) were placed in a specimen holder ring made of PMMA with 25 mm diameter and 8.5 mm height, rotating at 5 degrees per minute during analysis.

To determine the relative amounts of the various crystalline allomorphs of cellulose (CI and CIII) as well as the level of AC in a sample, a series of standards were produced as described previously in the main paper and further analyzed by XRD. As the CI and CIII standards contained a relatively high content of AC, it was required to remove the amorphous portion of the XRD spectra, thereby reproducing spectra correspondent to 100% crystalline CI and CIII. For this purpose, AC standard (PASC) was used in a technique designated by amorphous subtraction method (ASM).^{1,2} Figure S5 shows how the ASM method was applied to the CI and CIII standards. The yellow area, representing the AC spectrum, was subtracted from the XRD spectra of CI and CIII, generating new XRD spectra representative of 100% crystalline CI and CIII.

These XRD spectra representing 100% CI and CIII were further used in peak deconvolution of several ammonia-pretreated samples produced in this study. For illustration, Fig. S6 shows a

sample containing a mixture of AC, CI and CIII, which was deconvoluted using standard spectra of CI, CIII and AC. The deconvolution was performed using the following equation:

$$\text{Model XRD Spectra} = \alpha \cdot AC + \beta \cdot CI + \gamma \cdot CIII \quad (1)$$

Where,

AC = amorphous cellulose spectra; CI = 100% cellulose I standard spectra; $CIII$ = 100% cellulose III standard spectra. The coefficients α , β and γ control the proportion of each crystal in the mixture.

The coefficients α , β and γ from the model XRD spectrum were determined using the least squares method. The resulting model XRD spectra were further evaluated for statistical significance, showing in all cases P values of 0.00 and R^2 values above 0.99. In Fig. S6 is possible to observe an example of a model curve (in red) fitting the XRD spectra of a sample containing unknown composition of CI, CIII and AC. The composition of a designated sample containing CI, CIII, and AC was analyzed based on the relative area occupied by each standard XRD spectrum after deconvolution. For all the model fits reported in this manuscript, R^2 values were always higher than 0.99, demonstrating the ability of the model to fit XRD spectra obtained for the various conditions.

Peak deconvolution methods have been used in the literature to calculate the crystallinity index of cellulose samples,^{1,3-5} however they are usually performed summing a combination of Gaussian, Lorentzian or Voigt functions to fit XRD spectra of the sample. However, multiple curves are required to describe a mixture of various cellulose allomorphs, and the high number of degrees of freedom increases the number of possible combinations of intensity for the curves that describe the XRD spectrum of the sample. The method described herein, eliminates this problem in great extent, as the ratio between each peak is maintained constant within the standard XRD spectrum of CI, CIII, and AC. Therefore, the method produces consistent results, favoring our analysis, which is will be mainly a relative comparison between samples as opposed to a discussion about absolute values.

M6. FT-IR spectroscopy analysis

Fourier transform infrared (FTIR) spectra for a small set of pretreated celluloses (analyzed as is without additional drying or pelletting) was recorded using a Thermo Nicolet iZ10 spectrometer equipped with an ATR probe at the Forest Product Labs (Madison, WI). Spectra were recorded in the spectral region 4000 to 600 cm^{-1} , with 4 cm^{-1} resolution and accumulation of 128 scans per sample. Relevant results from the analysis are shown in Figure S7.

M7. FT-Raman spectroscopy analysis

A MultiRam FT-Raman spectrometer (Bruker) was used to collect Raman spectra for some pretreated cellulose samples at the Forest Product Labs (Madison, WI). The FT-Raman spectrometer was equipped with a 1064-nm 1000-mW Nd:YAG laser. For Raman analysis, cellulose pellets were first prepared from either lyophilized or air-dried samples prior to analysis. In most cases, spectra with high signal-to-noise (S/N) ratios was obtained upon using a 660 mW laser power setting and collecting over 512 scans per sample. Bruker OPUS 7.2 software was used to process the spectral data which involved selection of a spectral region, background correction, and if needed normalization of spectra typically at 1096 cm^{-1} . Background correction was

performed using a 64 points OPUS “rubber band option”. The spectra were then converted to ASCII format and exported to Microsoft Excel for plotting/analysis. In some cases, the crystallinity index ($\text{CrI}_{\text{Raman}}$) based on the relative Raman spectral intensity at 380 vs. 1096 cm^{-1} was determined using a previously published method and available $\text{CrI}_{\text{Raman}}$ formula.^{6,7} Relevant results from the analysis are shown in Figure S2.

To study the reversion of CIII into CI, enzymatic hydrolysis was carried out for the $-30 \text{ }^{\circ}\text{C}$ ammonia treated sample and the residual digested sample was analyzed by FT-Raman. Since enzymatic hydrolysis was carried out at $50 \text{ }^{\circ}\text{C}$, it was possible that some reversion of CIII to CI could have taken place during the course of enzymatic hydrolysis. However, we suspect that higher temperatures (close to $90\text{--}100 \text{ }^{\circ}\text{C}$ as reported by Lewin and others using boiling water) are likely necessary to full revert the low crystallinity CIII sample back into CI. To test this hypothesis, we ran experiments on the $-30 \text{ }^{\circ}\text{C}$ sample before and after incubation at $50 \text{ }^{\circ}\text{C}$ (either with or without a fungal cellulase cocktail added to the aqueous solution). Briefly, as described in the methods section, enzymatic hydrolysis was conducted at $50 \text{ }^{\circ}\text{C}$ for two days using a commercial cellulase cocktail at 5 mg/g glucan loading. Samples without any enzymes were also incubated in buffer for the same extent of time as a control. Residual cellulose samples with cellulase enzymes were washed extensively to remove bound enzymes before vacuum lyophilization to dry the sample followed by pelletization prior to FT-Raman analysis. Relevant results from the analysis are shown in Figure S2. We do not see a significant reversion of the $-30 \text{ }^{\circ}\text{C}$ sample based on the key spectral features of CIII still clearly preserved if the sample is incubated in an aqueous buffer alone. Marginal differences in the spectra are seen if the sample is incubated along with enzymes (see relative peak intensity of the 350 to 380 cm^{-1} peaks or use 1096 peak intensity to normalize for other peaks). Therefore, we can conclude that the $-30 \text{ }^{\circ}\text{C}$ sample shows no significant reversion during the course of enzymatic hydrolysis. Nevertheless, this work highlights the possible minor reversion of CIII if enzymatic hydrolysis is conducted at higher temperatures and researchers should consider monitoring their residual samples after hydrolysis to check for possible reversion.

Peak assignments of the vibrational spectrum of cellulose have been described elsewhere and have been summarized in Fig. S2.^{7,8} Briefly, $250\text{--}550 \text{ cm}^{-1}$ region for cellulose has predominant group motions attributed to skeletal-bending modes involving C-C-C, C-O-C, O-C-C, and O-C-O internal bond coordinates. The $550\text{--}750 \text{ cm}^{-1}$ region corresponds to mostly out-of-plane bending modes involving C-C-C, C-O-C, O-C-O, C-C-O, and O-H internal bond coordinates. The peaks around 900 cm^{-1} are shown to involve bending of H-C-C and H-C-O bonds localized at C-6 atoms of the hydroxymethyl group. The $950\text{--}1200 \text{ cm}^{-1}$ region corresponds to mostly stretching motions involving C-C and C-O internal bond coordinates. The $1200\text{--}1500 \text{ cm}^{-1}$ region corresponds to mostly bending motions involving H-C-C, H-C-O, H-C-H, and C-O-H internal bond coordinates. The region of $1400\text{--}1500 \text{ cm}^{-1}$ for cellulose has been shown to be particularly sensitive to the CH_2 scissor bending modes that are sensitive to the Trans-Gauche or TG (1480 cm^{-1}) and Gauche-Trans or GT (1460 cm^{-1}) conformations of the hydroxymethyl group.⁷

M8. Type-A CBM relative binding to cellulose-III allomorphs of varying crystallinity

Green Fluorescent Protein (GFP) labeled carbohydrate-binding module CBM3a (from *Ruminoclostridium thermocellum*) was prepared, as described elsewhere,⁹ to characterize binding of model type-A CBMs to cellulose-III samples of varying crystallinity. Briefly, the binding assays were carried out in a 1.5 mL micro centrifuge tubes, as described in detail elsewhere,¹⁰ using 5 mg

of cellulose suspended in 1 mL of 10 mM MES (pH 6.5) containing 50 μ g/mL equivalent GFP-CBM3a protein concentration. The mixtures were inverted at 5 rpm in a rotating carousel hybridization oven (VWR, Batavia, IL) at 25 °C for 1 h to allow binding equilibrium to be achieved. Free protein concentration in the supernatant was estimated using GFP fluorescence and used to estimate the total percentage of cellulose-surface bound protein based on the solid depletion adsorption method.¹¹ Relevant results from the analysis are shown in Figure S3.

Supporting Information (SI) Result Tables and Figures:

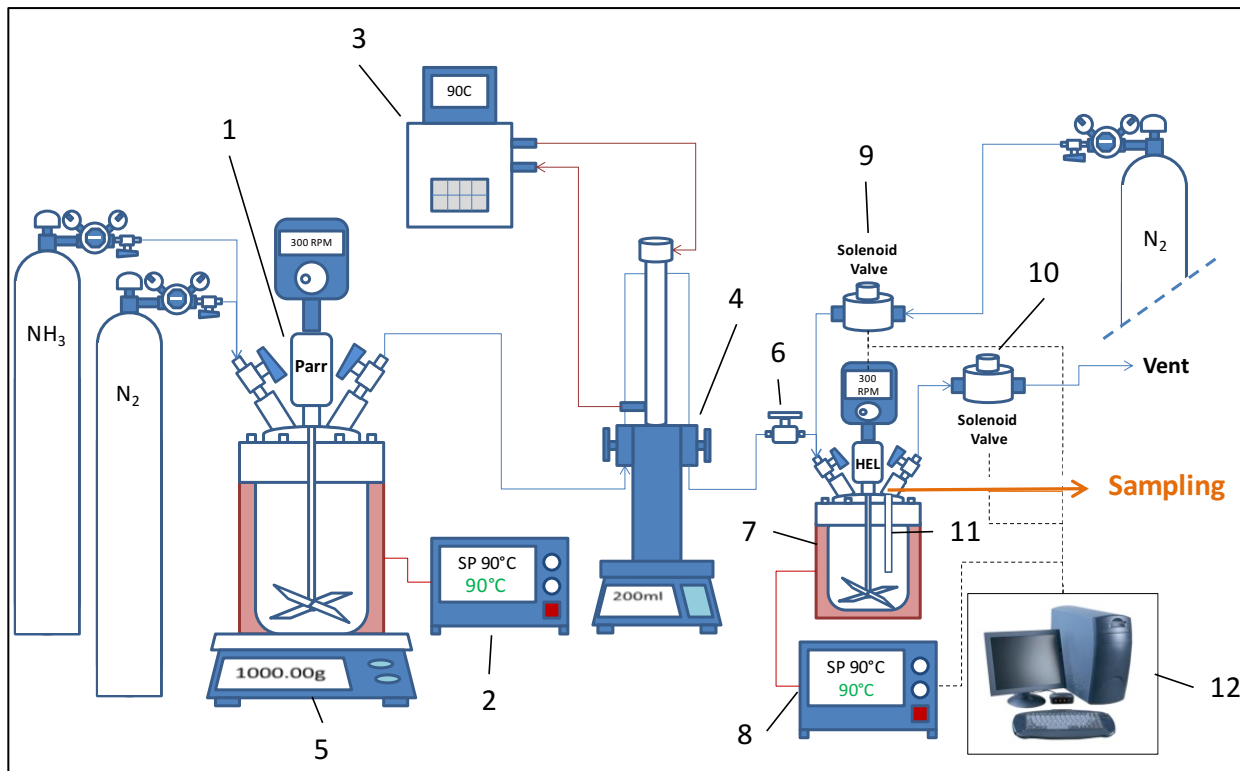
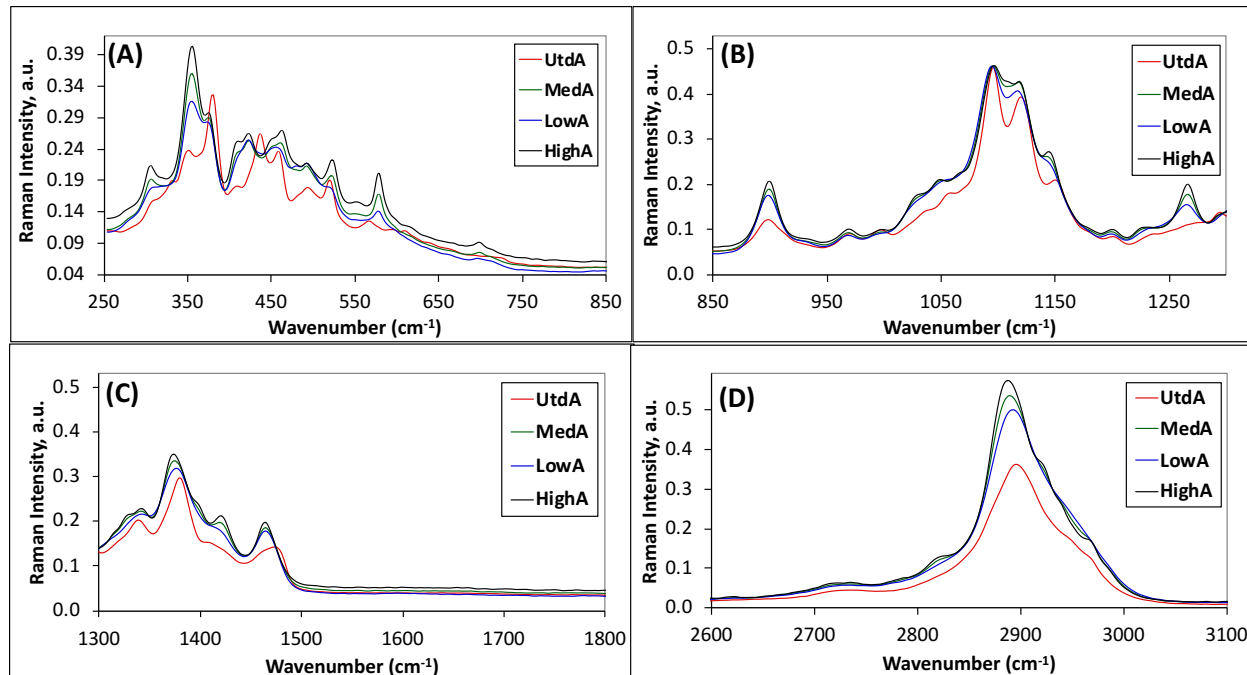


Figure S1. Instrumentation and pretreatment reactor setup for facilitating conversion of CI to CIII in a controlled-manner. Here, 1) High-pressure mixing vessel and mantle used to preheat ammonia to set-point temperature; 2) Temperature controller for ammonia preheating vessel; 3) Water circulator used to heat the syringe pump to reaction set-point temperature; 4) Syringe pump to pump the desired volume of ammonia; 5) Balance to confirm the delivery of the desired ammonia loading; 6) Backpressure regulator; 7) High-pressure stirred reaction vessel and mantle for cellulose III conversion; 8) Temperature controller for reaction vessel; 9) Solenoid valve for pressure control (nitrogen inlet); 10) Solenoid valve for pressure control (nitrogen outlet), also used for venting the system; 11) Dip tube sampling port; and 12) computer controls and data logging.



Based on Normalized Intensity				Key peak (P) and shoulder (S) features				Class of vibrational states	
Wavenumber	UtdA	MedA	LowA	HighA	UtdA	LowA	MedA	HighA	Class of vibrational states
309	0.156	0.182	0.180	0.173	S	S	P	P	CCC ring
332	0.19	0.18	0.19	0.17	P				CCC ring
350	0.23	0.32	0.30	0.31	S	P	P	P	CCC ring
355	0.23	0.35	0.32	0.34	S	P	P	P	CCC ring
375	0.28	0.28	0.28	0.25	P	S	S	S	
380	0.32	0.25	0.25	0.22	P	S	S	S	
425	0.20	0.24	0.25	0.22	P	P	P	P	
438	0.25	0.22	0.23	0.19	P				
458	0.23	0.24	0.24	0.22	P	S*	S	S	CCC, CCO ring
463	0.20	0.24	0.23	0.22	P	P	P	P*	CCC, CCO ring
519	0.19	0.19	0.18	0.18	P	S*	P	P	CCC ring/glycoside
566	0.12	0.13	0.13	0.13	P				
581	0.11	0.15	0.14	0.16	P	P*	P*	P*	
701	0.07	0.07	0.07	0.08	S	P	P*		OH out of plane
726	0.07	0.06	0.06	0.06	P	S			
899	0.12	0.18	0.18	0.17	P	P*	P*	P*	HCC/HCO bending at C6
971	0.09	0.09	0.09	0.08	P	P	P	P	
996	0.10	0.09	0.09	0.08	P*	S	S	P*	
1036	0.14	0.17	0.18	0.15	P*	P			CO pri alcohols
1057	0.18	0.20	0.21	0.17	P*	P			CO sec alcohols
1098	0.43	0.44	0.45	0.38	P	P	S	S	Asymmetric glycoside
1121	0.39	0.40	0.40	0.35	P	P	S	S	Symmetric glycoside
1146	0.20	0.25	0.24	0.23	P	S	S	S	
1266	0.11	0.17	0.16	0.17	S	P	P	P	CH2 vibration
1293	0.13	0.13	0.13	0.11	P	S	S	S	CH2 bending/vibration
1339	0.20	0.21	0.22	0.19	P	S	S	P	
1374	0.27	0.32	0.32	0.29	P	P	P	P	
1379	0.29	0.31	0.31	0.27	P	S*	S*	S	
1422	0.13	0.19	0.17	0.17	S	S	P	P	
1464	0.13	0.18	0.18	0.16		P	P	P	
1476	0.14	0.13	0.13	0.11	S				
2818	0.08	0.11	0.11	0.10	S	S	S	P	
2890	0.34	0.52	0.50	0.48	P	SHIFTS TO 2885 from L to H			
3296	0.03	0.03	0.03	0.02	P	SHIFTS FROM LOW TO HIGH			
3347	0.04	0.03	0.03	0.02	P	SHIFTS FROM LOW TO HIGH			

Skeletal bending CCC, COC, OCC, OCO

Stretching CH, CH₂, & OH group vibrations

CCC, COC, OCC, COO bending & OH out of plane

HCC/HCO bending at C6 position

CO, CC stretching; Coupled motions of glucose rings

HCC, HCO, HCH, COH bending & OH in plane

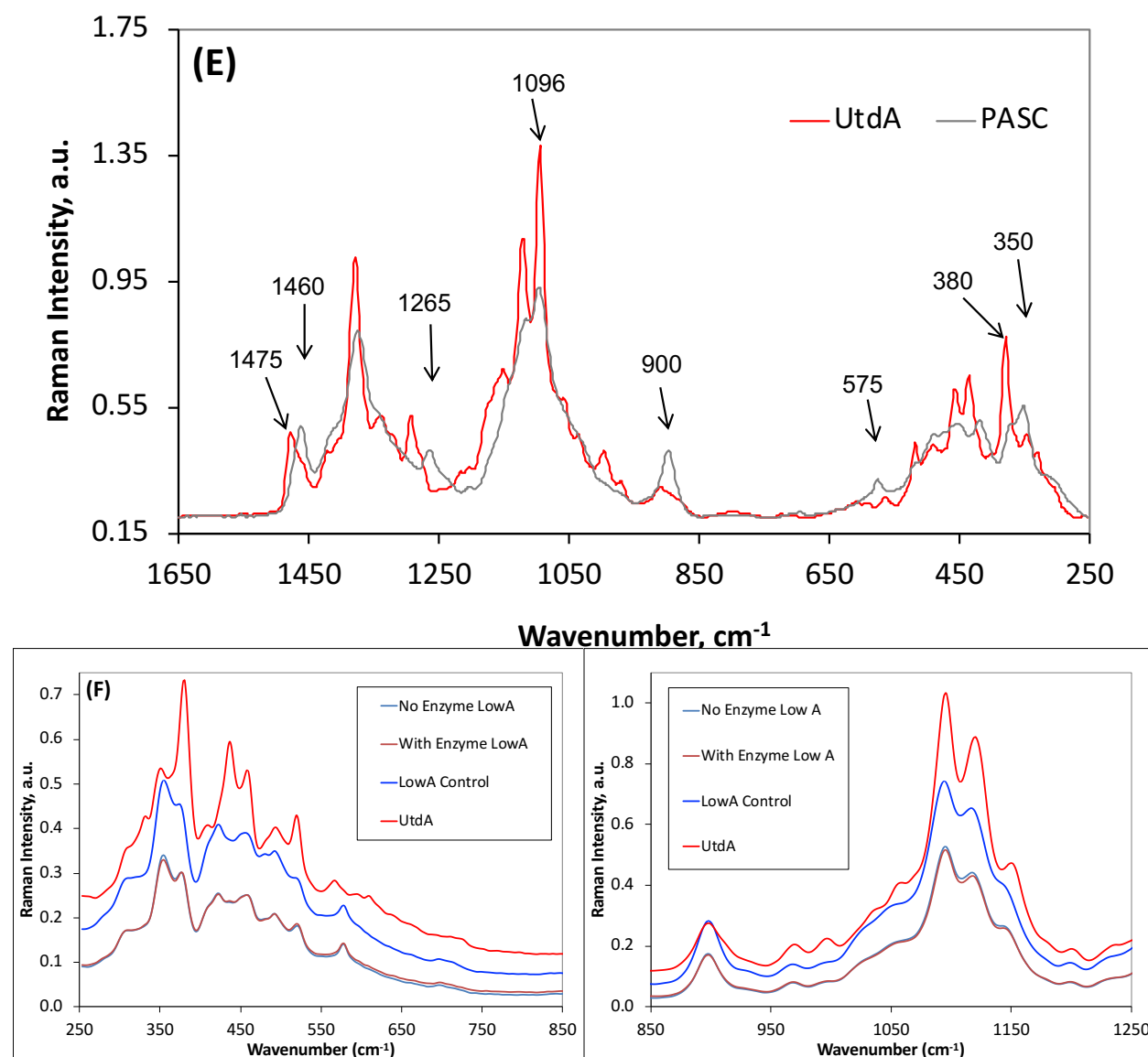


Figure S2. FT-Raman spectra of Avicel PH-101 treated with ammonia at varying reaction temperatures (A-D) and phosphoric acid to produce PASC (E). Table below figures S2 (A-D) summarizes the key spectral features seen for all samples and some critical spectral peak (P) or shoulder (S) bands assignments based on published work.^{6,7} Here, reaction temperature was at -30 °C (LowA in blue color), at 25 °C (MedA in green color), and at 90 °C (HighA in black color). Control untreated Avicel-PH101 or cellulose I spectra is shown as well (UtdA in red color). PASC sample was lyophilized prior to analysis (PASC in grey color). Low temperature ammonia treated samples had some spectra features that resembled highly disordered amorphous cellulose (like lyophilized PASC as shown in E) as well as features that resembled cellulose-III. Low temperature ammonia treated samples spectra was also measured before and after enzymatic hydrolysis to confirm minimal reversion to CI took place during the course of enzymatic hydrolysis at 50 °C in aqueous buffer (F). The -30 °C (LowA) was either incubated with enzymes or without any enzymes. Relative extent of highly ordered cellulose III formation can be estimated based on the relative peak intensity of 380 and 350 cm^{-1} .^{8,12,13}

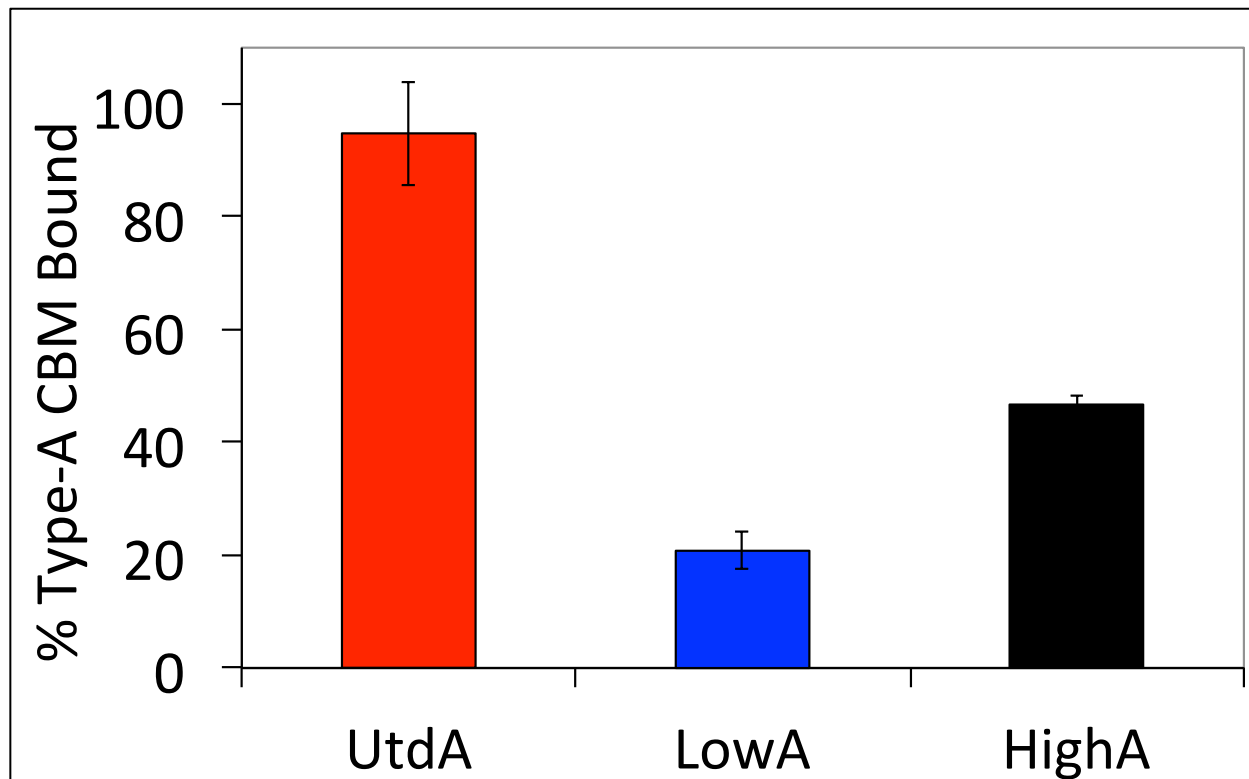


Figure S3. Relative binding capacity of GFP-labeled carbohydrate binding module (CBM3a) cellulolytic protein to Avicel PH-101 treated with ammonia at -30 °C (LowA in blue color) and 90 °C (HighA in black color) is shown here to determine the relative binding accessibility of cellulolytic enzymes to each respective substrate. Control untreated Avicel-PH101 or cellulose I results are shown here as well (UtdA in red color). The results here clearly indicate that the structurally more ordered and crystalline native CI (red) and high crystallinity CIII (black) both show increased CBM binding compared to the low crystallinity CIII (blue) sample. Detailed characterization of CBM binding to cellulose-III allomorphs is to be published elsewhere.

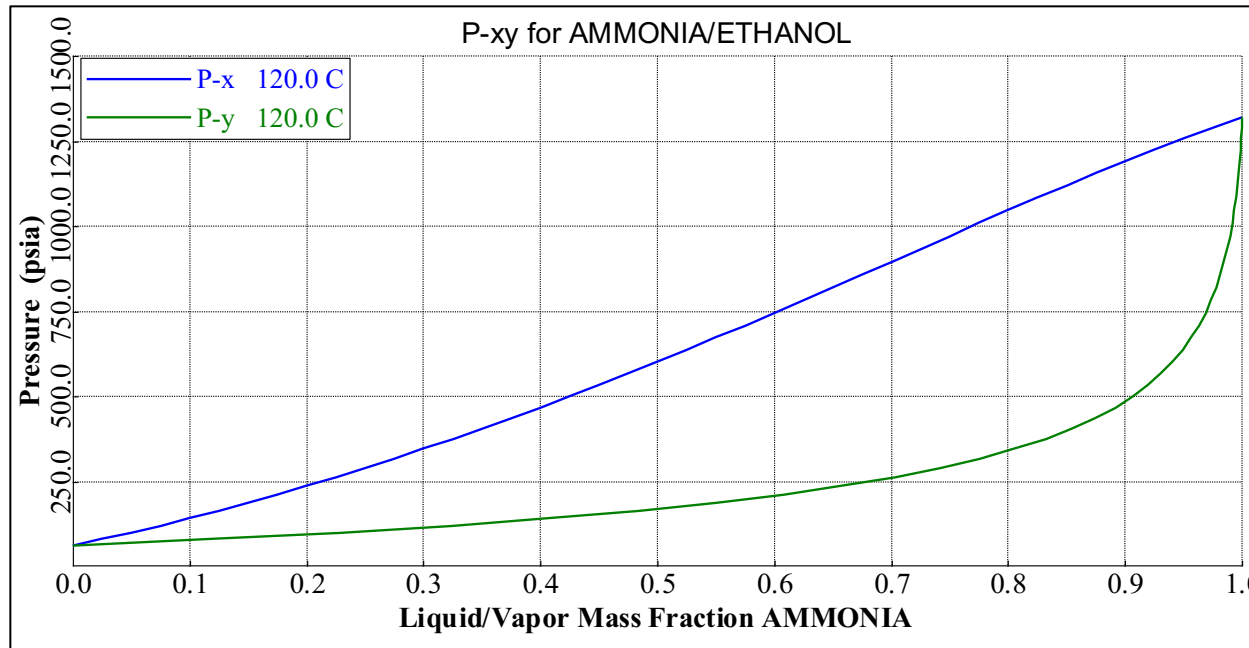


Figure S4. Vapor-liquid equilibrium (VLE) pressure-composition curves (P-xy) for ammonia/ethanol mixture at 120 °C is shown here. The P-x and P-y curves were predicted using the standard Non-Random Two Liquid (NRTL) thermodynamic model after estimating the missing parameters using UNIFAC model in Aspen Plus (v.7.1) software. This VLE curve can predict the thermodynamic VLE state of a two component mixture (ammonia/ethanol) as a function of pressure at desired temperature of 120 °C. Briefly, any point that lies above the blue P-x line would be in the liquid state, while any point below the green P-y line would be in the vapor. Any point between the two lines would be in a VLE equilibrium and the composition of the two phases can be estimated using an isobaric tie line and this VLE phase diagram. The main idea behind presenting this figure is to provide a theoretical basis to the choice of the operating pressure necessary for a 60% (by mass) ammonia/ethanol mixture necessary to achieve a liquid phase necessary to convert cellulose-I to cellulose-III supporting experiment results presented in the paper.

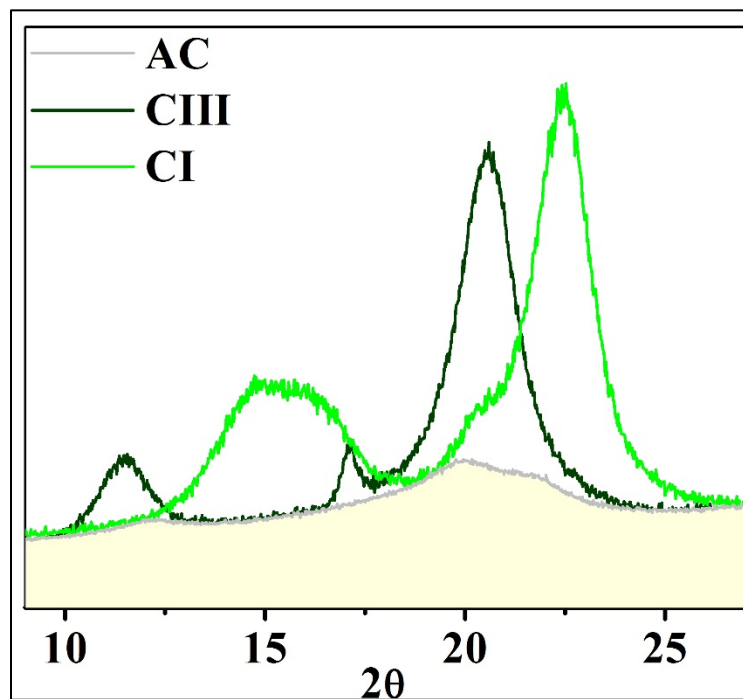


Figure S5. Illustrative example of XRD spectra of cellulose I (CI), cellulose III (CIII) and amorphous cellulose or PASC (AC) standards. Amorphous subtraction method was applied to CI and cellulose CIII standards used in this study. The yellow area was subtracted from the XRD spectra of CI and CIII standards to recreate a 100% crystalline CI and CIII spectra used for subsequent XRD spectra deconvolution.

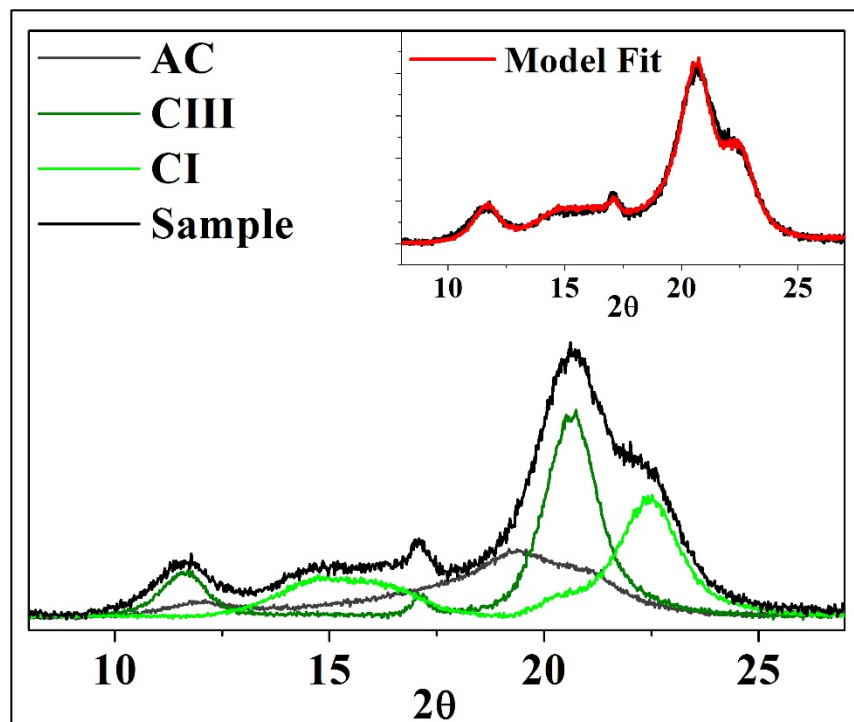


Figure S6. Illustrative example of XRD peak deconvolution applied to an ammonia pretreated sample containing a mixture of disordered or amorphous cellulose (AC), cellulose I (CI), and cellulose III (CIII). The model fit for the spectra (red line), contrasting with the sample XRD spectra (black line), is presented in the top right as inset.

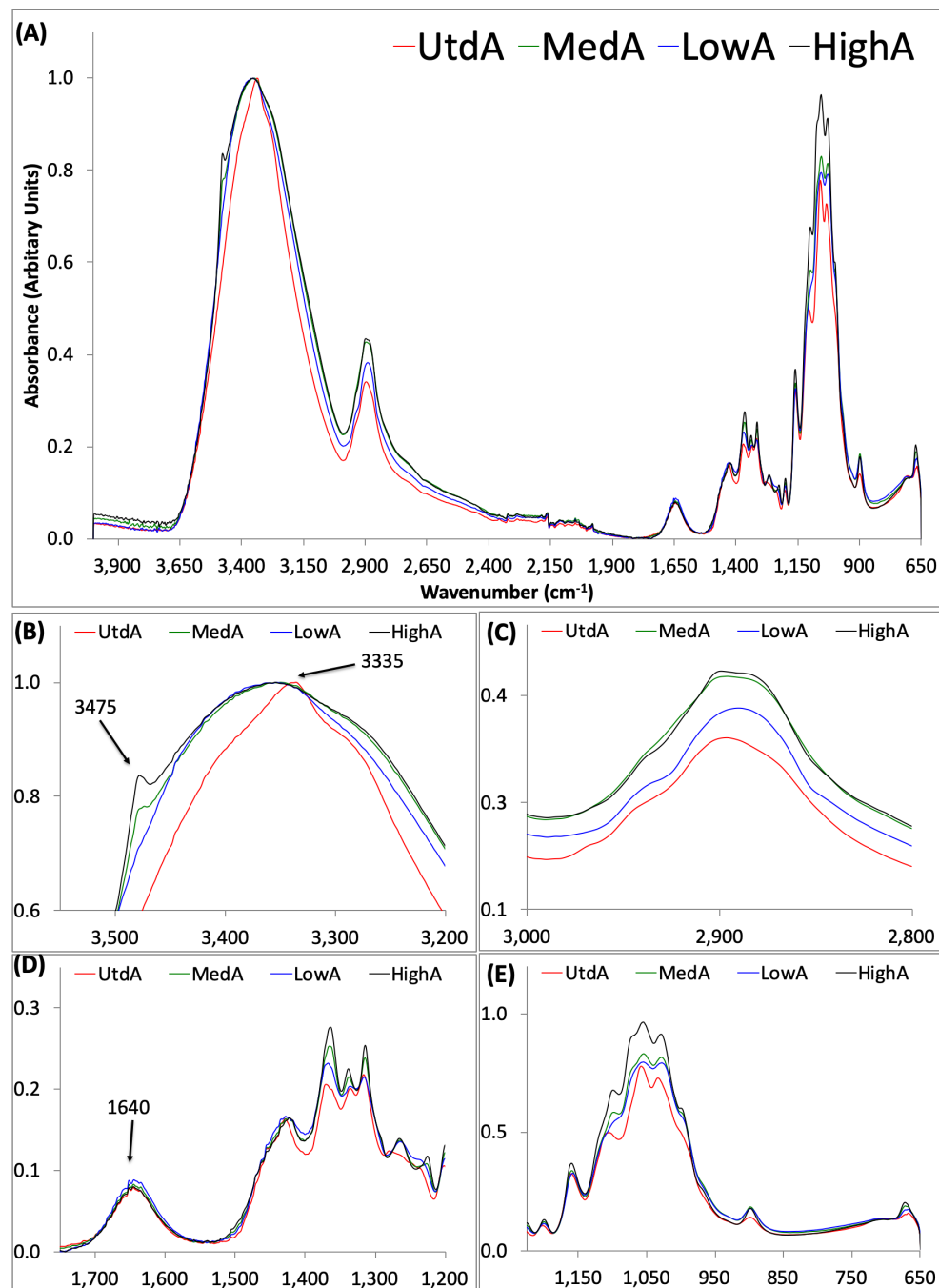


Figure S7. FTIR-ATR spectra of Avicel PH-101 treated with ammonia at varying reaction temperatures are shown here (A). Here, reaction temperature was at -30 °C (LowA in blue color), at 25 °C (MedA in green color), and at 90 °C (HighA in black color). Control untreated Avicel-PH101 or cellulose I spectra is shown as well (UtdA in red color). Details of original spectra in (A) are shown in magnified spectral insets (C) to (E) highlighting critical differences.

Table S1. Impact of pretreatment temperatures on cellulose III formation and its enzymatic saccharification rate. Here statistics for data reported in Figure 3 and 4 are shown. All XRD analyses were carried out in duplicate with mean values for total crystalline (as CI, CIII) or amorphous cellulose (as AC) peak areas are reported here as %XRD Area. Here XRD analyses data for the samples recovered after 30 min total pretreatment time alone is provided for all pretreatment temperatures tested. Standard deviations ($\pm 1\sigma$) for reported mean values are shown here. All hydrolysis assays were carried out in duplicate with mean values for glucan-to-glucose conversion reported here in the right-hand side column. Standard deviations ($\pm 1\sigma$) for reported mean values are shown here.

Substrate Type	AC (%XRD Area)	CI (%XRD Area)	CIII (%XRD Area)	%Glucan Conversion
Avicel	49.9 % \pm 1.7 %	50.1 % \pm 1.7 %	-	25.9 % \pm 0.1 %
PASC	100 %	-	-	54.3 % \pm 0.1 %
-30 °C NH ₃	-	-	-	30.2 % \pm 0.5 %
25 °C NH ₃	58.6 % \pm 1.6 %	0.0 % \pm 0.0 %	41.4 % \pm 1.6 %	32.4 % \pm 0.6 %
90 °C NH ₃	50.9% \pm 2.3 %	0.0 % \pm 0.0 %	49.1 % \pm 2.3 %	39.2 % \pm 0.2 %

Additional References

- (1) Park, S.; Baker, J.; Himmel, M.; Parilla, P.; Johnson, D. Cellulose Crystallinity Index: Measurement Techniques and Their Impact on Interpreting Cellulase Performance. *Biotechnol. Biofuels* **2010**, *3* (1), 10.
- (2) Ruland, W. X-Ray Determination of Crystallinity and Diffuse Disorder Scattering. *Acta Cryst* **1961**, *14*, 1180–1185.
- (3) Hult, L.; Iversen, T.; Sugiyama, J. Characterization of the Supramolecular Structure of Cellulose in Wood Pulp Fibres. *Cellulose* **2003**, *10*, 103–110.
- (4) Garvey, C. J.; Parker, I. H.; Simon, G. P. On the Interpretation of X-Ray Diffraction Powder Patterns in Terms of the Nanostructure of Cellulose I Fibres. *Macromol. Chem. Phys.* **2005**, *206* (15), 1568–1575 DOI: 10.1002/macp.200500008.
- (5) He, J.; Cui, S.; Wang, S.-Y. Preparation and Crystalline Analysis of High-Grade Bamboo Dissolving Pulp for Cellulose Acetate. *J Appl Polym Sci* **2008**, *107*, 1029–1038.
- (6) Agarwal, U.; Reiner, R.; Ralph, S. Cellulose I Crystallinity Determination Using FT-Raman Spectroscopy: Univariate and Multivariate Methods. *Cellulose* **2010**, *17* (4), 721–733.
- (7) Agarwal, U. P. 1064 Nm FT-Raman Spectroscopy for Investigations of Plant Cell Walls and Other Biomass Materials. *Front. Plant Sci.* **2014**, *5*, 490 DOI: 10.3389/fpls.2014.00490.
- (8) Wiley, J. H.; Atalla, R. H. Band Assignments in the Raman Spectra of Celluloses. *Carbohydr. Res.* **1987**, *160* (null), 113–129 DOI: 10.1016/0008-6215(87)80306-3.
- (9) Whitehead, T. A.; Bandi, C. K.; Berger, M.; Park, J.; Chundawat, S. P. S. Negatively Supercharging Cellulases Render Them Lignin-Resistant. *ACS Sustain. Chem. Eng.* **2017**, *5* (7), 6247–6252 DOI: 10.1021/acssuschemeng.7b01202.
- (10) Lim, S.; Chundawat, S. P. S.; Fox, B. G. Expression, Purification and Characterization of a Functional Carbohydrate-Binding Module from Streptomyces Sp. SirexAA-E. *Protein Expr. Purif.* **2014**, *98*, 1–9 DOI: 10.1016/j.pep.2014.02.013.
- (11) Gao, D.; Haarmeyer, C.; Balan, V.; Whitehead, T. A.; Dale, B. E.; Chundawat, S. P. Lignin Triggers Irreversible Cellulase Loss during Pretreated Lignocellulosic Biomass Saccharification. *Biotechnol. Biofuels* **2014**, *7* (1), 175 DOI: 10.1186/s13068-014-0175-x.
- (12) Chundawat, S. P. S.; Donohoe, B. S.; Sousa, L.; Elder, T.; Agarwal, U. P.; Lu, F.; Ralph, J.; Himmel, M. E.; Balan, V.; Dale, B. E. Multi-Scale Visualization and Characterization of Plant Cell Wall Deconstruction during Thermochemical Pretreatment. *Energy Environ. Sci.* **2011**, *4* (3), 973–984 DOI: 10.1039/C0EE00574F.
- (13) Atalla, R. J.; Vanderhart, D. L. Studies on the Structure of Cellulose Using Raman Spectroscopy and Solid State ¹³C-NMR. In *Institute for Paper Chemistry (IPC Technical Paper Series 217)*; chemistry, I. for paper, Ed.; 1987; Vol. IPC Techn.